Response to Comments by Anonymous Referee #1

General comments:

This manuscript investigated the emissions of various primary pollutants and photochemical evolution from burning three types of agricultural residues (corn, rice and wheat straws) by using a 30m^3-smog chamber. The experimental design is reasonable, the results are reliable, and the conclusions are convincing. Considering the rare information on primary emissions and photochemical evolution of agricultural residues burning, the original data presented in this manuscript are very important for comprehensibly understanding the impact of the burning on the air quality, especially in China. The manuscript is well organized, and hence this reviewer recommends the manuscript be published in the journal.

Response: We would like to thank the referee # 1 for the positive comments. We have revised our manuscript after carefully reading the following constructive suggestions. We believe that the changes considerably helped to improve the quality of the manuscript.

Specific comments:

[1] Both biomass burning and domestic coal combustion have been recognized to make evident contribution to deteriorating regional air quality especially in North China. If the authors had compared with the emission strengths between the biomass combustion and domestic coal combustion, the result would be more attractive. The authors only compared with the SO_2 emission factors between the biomass burning and coal cake combustion, however the emission factor of coal cake might be outdated, because raw bituminous is currently prevailing for cooking and heating in rural areas. The emission factors of various pollutants from combustion of raw bituminous in domestic stove have been reported (e.g. SO_2 emission factors of 4.16-1.36 g SO_2 kg^{-1}, Du, Q. et al. (2016), An important missing source of atmospheric carbonyl sulfide: Domestic coal combustion, Geophys. Res. Lett., 43(16), 8720–8727, doi:10.1002/2016GL070075; NMHCs (57 species) average emission factor of 2981.1 mg kg^{-1}, Liu et al.(2017), Emission of volatile organic compounds from domestic coal stove with the actual

alternation of flaming and smoldering combustion processes, Environmental Pollution 221, 385-391). Although the emission factors of SO_2 from the burning of corn and wheat straw is about 3-6 times less than that of coal combustion and of NMHCs is comparable to each other, the emissions of these pollutants from the biomass burning might largely exceed those from domestic coal combustion because the amount of the biomass burning might be one magnitude greater than that of domestic coal consumption in China. Therefore, greater attention should be paid on the emission of biomass burning for improving the air quality in China.

Response: We agree that the comparison of primary emissions between agricultural residues burning and domestic coal combustion would help policy makers for the control of air pollution. As suggested, we have updated emission factors for coal combustion in the latest literatures, and added the following words in the revised "Conclusions" part:

"Both agricultural residues burning and domestic coal combustion have been recognized to contribute substantially to the deteriorating regional air quality especially in rural areas of China (Pan et al., 2015; Liu et al., 2016; Zhu et al., 2016). The emission factors of the speciated NMHCs, PM, NO_x, CO and SO_2 from combustion of raw bituminous, which is currently prevailing for cooking and heating in rural areas, have been reported to be 0.56-5.40, 25.49±2.30, 0.97±0.03, 208±5 and 2.43-5.36 g kg^{-1}, respectively (Du et al., 2016; Li et al., 2016; Liu et al., 2017). Annually burned crop residues and domestic coals were estimated to be 160 Tg (Li et al., 2016) and 99.6 Tg (NBSPRC, 2014) in China. Therefore, with the emission factors of the speciated NMHCs (2.47-5.04 g kg^{-1}), PM (3.73-6.36 g kg^{-1}), NO_x (1.47-5.00 g kg^{-1}), CO (46.1-63.5 g kg^{-1}) and SO_2 (0.07-0.99 g kg^{-1}) measured for agricultural residues burning in this study, agricultural residues burning might emit more NMHCs and NO_x, but less primary PM, CO and SO_2 than domestic coal burning on a national scale."

[2] The concentration of OH radical indirectly obtained by tracing the first order decay rate of toluene should represent its average concentration during the whole irradiation, why did you use the OH exposure of (1.87-4.97)×10^{10} molecule cm^{-3} s? Are your sure

the lifetime of OH radical in the chamber is only 1s? I suggested to use the unit of average concentration (1.87-4.97)×10^{10} molecule cm^{-3}.

Response: In fact, the average OH concentration in this manuscript was calculated every 2 minutes by continuous monitoring of toluene concentration through PTR-TOF-MS, thus the average "OH exposure" every 2 min was calculated as the product of average OH concentration and the time interval. OH exposure, indicating the atmospheric oxidation power that a pollutant undergoes, is a parameter that has been widely used in the chamber studies (e.g., Hennigan et al., 2010; Tiitta et al., 2016; Tkacik et al., 2017). In the revised manuscript, we have revised the manuscript to include this detailed information about how the average OH concentration was calculated: "The decay of toluene measured by PTR-TOF-MS was used to derive the average OH radical concentrations for every 2 min during each experiment, and the integrated OH exposure was calculated as the product of the OH concentration and the time interval."

[3] Although the contribution of the 20 NMOGs to the SOA only accounted for 5-27.3% of the observed SOA mass, the increase of the SOA mass might not solely be ascribed to the aqueous-phase oxidation of alkenes, because the oxidation of the POM with more oxygen can also make evident contribution.

Response: The possible contribution from the oxidation of POM has been included in the revised manuscript, and some other reasons for the discrepancy have also been added:

"It is noted that although over 80 VOCs species were quantified by the GC-MSD/FID and the PTR-TOF-MS in this study, only 20 species among them were taken into the SOA prediction because of the lack of published data for SOA yields. The unaccounted VOC species might be a reason for the discrepancy. On the other hand, as indicated by Deng et al. (2017), SOA yields obtained from chamber studies in purified air matrix might be lower than that in real ambient air matrix. Consequently, using SOA yields from studies in purified air matrix might also under predict SOA yields in the complex biomass burning plume matrix. Moreover, oxidation of particulate organic matters

(POM), like semi-volatile organic compounds (SVOC) and intermediate volatility organic compounds (IVOC), would also contribute substantially to SOA formation (Presto et al., 2009; Zhao et al., 2014), yet this is not accounted for in our prediction..”

[4] (Page 16, line 366-368) The two OA enhancement ratios reported were evidently less than those determined in this study, why did you concluded that the OA enhancement ratios determined were higher than those (0.7-2.9) for the combustion of vegetation, and comparable to those (0.7-6.9) for wood burning?

Response: The OA enhancement ratio in our study should be 2.4-7.6 rather than 2.4-76 in this sentence. We are quite sorry for this typo and have corrected it in the revised manuscript.

Response to Comments by Anonymous Referee #2

General comments:

[1] Open burning of agricultural residues is a large source of both primary and secondary air pollutants in Asia and in China. Although many studies have been carried out, emission factors reported in previous study vary substantially due to differences in fuel types and combustion conditions. In addition, few studies have been performed to investigate the SOA formation from agricultural residues. To better understanding the effects of biomass burning on both primary and secondary pollution, this study comprehensively characterizes the primary emissions and determines SOA formation potential of emissions from the major agricultural residues in China, including corn, rice and wheat straws. Results from study would significantly improve our understanding the effects of agricultural residues on air quality. In addition, the results from this study also provide constraints on estimation of the contributions of other sources to air pollution. Publication is recommended after the following comments and concerns are addressed.

Response: We would like to thank the referee #2 for the positive comments. We have revised our manuscript with the constructive comments and suggestions below. We believe that the changes considerably helped to improve the quality of the manuscript.

[2] Discussion is needed about why only a small fraction of observed SOA in this study was explained by the same set of speciated NMHCs which explain the majority of SOA in Bruns et al. (2016).

Response: Only a small fraction of observed SOA in this study was explained by the same set of speciated NMHCs, which explained the majority of SOA in Bruns et al. (2016). Recent studies indicated that IVOC and SVOC may contribute substantially to SOA. There might be at least SVOC in the biomass burning plumes. As indicated by the AMS data, CH-family or hydrocarbon was the major component of POA in the initial biomass burning plume (Figure 6a), after photo-oxidation they decreased in aged OA. This family of SVOC could be oxidized to form SOA. Considering the probable contribution from IVOC/SVOC to SOA formation, it would be reasonable that we observed the discrepancy. In the revised manuscript, we have added an explanation as below:

"It is noted that although over 80 VOCs species were quantified by the GC-MSD/FID and the PTR-TOF-MS in this study, only 20 species among them were taken into the SOA prediction because of the lack of published data for SOA yields. The unaccounted VOC species might be a reason for the discrepancy. On the other hand, as indicated by Deng et al. (2017), SOA yields obtained from chamber studies in purified air matrix might be lower than that in real ambient air matrix. Consequently, using SOA yields from studies in purified air matrix might also under predict SOA yields in the complex biomass burning plume matrix. Moreover, oxidation of particulate organic matters (POM), like semi-volatile organic compounds (SVOC) and intermediate volatility organic compounds (IVOC), would also contribute substantially to SOA formation (Presto et al., 2009; Zhao et al., 2014), yet this is not accounted for in our prediction."

[3] If the unexplained SOA is due to additional precursors, not quantified in this study, do these additional precursors substantially contribute to ozone formation? Based on the mass enhancement factor of 2.4-76 and the fact that similar emission factors for both measured NMHCs and PM, the amount of unmeasured NMHCs could be

dramatically larger than the measured ones. Is there any study measuring both total NMHCs and speciated NMHCs from biomass burning? The difference between total NMHCs and speciated NMHCs is a useful indicator of additional precursors.

Response: To our best knowledge, emissions of total NMHCs for agricultural residues burning has not yet been reported, and the amount of NMHCs quantified in this study (67 species) outnumbered those in other studies, such as 52 species measured by Li et al. (2009) and 56 species measured by Wang et al. (2014). We fully agree that measuring total NMHCs would help explaining the data. This is a very good suggestion and we are thinking how we can get it done in our future study. We think the additional precursors would also contribute substantially to ozone formation. A considerable amount of NMOG species, such like OVOCs, were detected by PTR-TOF-MS but not reported in this manuscript. Unmeasured NMHCs would also be oxidized to produce OVOCs, which may contribute substantially to ozone formation. For example, formaldehyde and acetaldehyde were among the most abundant NMOGs species detected by PTR-TOF-MS in the initial biomass burning plumes, and they also have relatively high maximum incremental reactivity (MIR) values (Carter, 2008). We have added the following statement in the revised manuscript:

"It is noted that oxygen-containing organic vapors in agricultural residues burning plumes could also have large ozone formation potentials. For example, the OFPs of formaldehyde and acetaldehyde for all experiments were 0.57-2.46 times of the 67 speciated NMHCs."

[4] This study has covered a wide range of measurements and compared with measurements in past studies. However, what we can learn from this study, other than emissions factors and OA enhancement factors, is not clearly stated. In other works, what makes this paper significant is not clearly stated.

Response: We think that this paper gives something new in three aspects:

(1) The emission factors were measured at ambient-level dilution ratios. Thus the errors caused by the evaporation of SVOCs from the particle phase to the gas phase were avoided.

(2) More than 60% of SOA mass cannot be explained by the known precursors.

(3) The f_{60} values in AMS spectrum of primary agricultural residues emissions were lower than those from field campaigns. The f_{60} value is often regarded as the biomass burning marker, so the present constraints on it need to be reconsidered.

Besides, as suggested by the anonymous referee #1, a comparison between agricultural residues burning and domestic coal burning in China were done to help policy makers in air pollution control especially in rural areas.

Specific comments:

[1] Line 136: define "purified dry air"

Response: The following sentences have been added to the revised manuscript: "The compressed indoor air is forced through an air dryer (FXe1; Atlas Copco; Sweden) and a series of gas scrubbers containing activated carbon, Purafil, Hopcalite and allochroic silica gel, followed by a PTFE filter to provide the source of the purified air. The purified dry air contains <1 ppb NO_x, O_3 and carbonyl compounds, <5 ppb NMHCs and no detectable particles with relative humidity <5%."

[2] Line 141-142: How was the water content determined?

Response: The following sentences have been added to the revised manuscript: "The water content of crop residues was measured by using the method recommended by Liao et al. (2004). The weight of straws were weighed before and after baking in a stove at 105℃ for 24 h, and the difference in weights was calculated to be the weight of the water in the crop residues. Water content was the quotient of the water weight and the whole weight of the straws."

[3] Line 152: change "diluted" to "dilute"

Line 155: change "correct" to "determine"

Line 188: change "this instrument alternated" to "the HR-TOF-AMS was operated by alternating"

Line 188: change "one" to "other"

Line 255: change “identified” to “quantified”

Response: Those errors have been corrected in the revised manuscript.

[4] Line 161: The section of “Instrumentation” is actually “Characterization of primary emissions and secondary organic aerosol”. In this section, I’d like to separate the description of the analysis of VOCs from other gases.

Response: We have separated the description of the analysis of VOCs from other gases. The first paragraph of section 2.2 has been corrected as follows:

“Commercial instruments were used for online monitoring of NO_x (EC9841T, Ecotech, Australia), NH_3 (Model 911-0016, Los Gatos Research, USA) and SO_2 (Model 43i, Thermo Scientific, USA). CH_4 and CO were analyzed offline using a gas chromatography (Agilent 6980GC, USA) coupled with a flame ionization detector and a packed column (5A molecular sieve 60/80 mesh, 3 m × 1/8 in) (Zhang et al., 2012), and CO_2 was analyzed using a HP 4890D gas chromatograph (Yi et al., 2007). The detection limits were all less than 30 ppbv for CH_4, CO and CO_2. The relative standard deviations (RSDs) of CO and CO_2 measurements were both less than 3% based on seven duplicate injection of 1.0 ppmv standards (Spectra Gases Inc, USA).

Volatile organic compounds (VOCs) were continuously measured using a proton-transfer-reaction time-of-flight mass spectrometer (PTR-TOF-MS; Model 2000, Ionicon Analytik GmbH, Austria). Calibration of the PTR-TOF-MS was performed every few weeks using a certified custom-made standard mixture of VOCs (Ionicon Analytik Gmbh, Austria) that were dynamically diluted to 6 levels (2, 5, 10, 20, 50 and 100 ppbv). Methanol, acetonitrile, acetaldehyde, acrolein, acetone, isoprene, crotonaldehyde, 2-butanone, benzene, toluene, o-xylene, chlorobenzene and α-pinene were included in the calibration mixture. Their sensitivities, indicated by the ratio of the normalized counts per second to the concentration levels of the VOCs in ppbv, were used to convert the raw PTR-TOF-MS signal to concentration (Huang et al., 2016). Quantification of the compounds that were not included in the mixture was performed by using calculated mass-dependent sensitivities based on the measured sensitivities (Stockwell et al., 2015). Mass-dependent sensitivities were linearly fitted for oxygen-

containing compounds and the remaining compounds separately. The decay of toluene measured by PTR-TOF-MS was used to derive the OH radical concentrations for every 2 min during each experiment, and the OH exposure was calculated as the product of the OH concentration and the time interval. Continuous monitoring of 20 SOA precursors (including 9 NMHCs and 11 oxygen-containing VOCs) from PTR-TOF-MS provided us with data to do the SOA prediction discussed in the Sect 2.3.5 and 3.3.2. Air samples were also collected from the chamber reactor using 2-Liter electro-polished stainless-steel canisters before and after smoke injection. In total 67 C_2-C_{12} NMHCs were measured (Table S1) using an Agilent 5973N gas chromatography mass-selective detector/flame ionization detector (GC-MSD/FID; Agilent Technologies, USA) coupled to a Preconcentrator (Model 7100, Entech Instruments Inc., USA), and analytical procedures have been detailed elsewhere (Wang and Wu, 2008; Zhang et al., 2010; Zhang et al., 2012). Results from GC-MSD/FID were used to quantify the emission factors of 67 NMHCs discussed in the Sect 3.1."

[5] Line 195: What is the AMS CE?

Response: AMS tends to underestimate the PM mass due to the transmission efficiency (Liu et al., 2007) and the AMS collection efficiency (Gordon et al., 2014). Besides, the black carbon, which is an important part of biomass burning particles, can hardly be captured because it doesn't rapidly vaporize in the vaporizer of AMS. These factors would lead to the discrepancy between the AMS data and SMPS data. AMS collection efficiency (CE) is calculated as the quotient of the total mass measure by AMS and the mass difference between the SMPS and the aethalometer. By dividing the AMS CE, the AMS data were corrected. Experiment-specific CEs ranged from 0.20 to 0.41 in this study.

[6] Line 217: Is the denominator of the equation (2) the same as the numerator? Why do you need two equations to calculate this fuel based emission factor?

Response: In fact, the carbon mass after burning will be distributed in both ash and in the gas phase, the equation (3) defines how to calculate the emission factor of the total

carbon mass in the gas phase (EF_C) by elemental and gravitational analysis. The equation (3) was often ignored in previous papers because the ash part was neglected while we want to clarify it explicitly here. In the right side of equation (2), the part $\frac{m_i}{\Delta[CO_2]+\Delta[CO]+\Delta[PM_C]+\Delta[HC]}$ means the mass ratio of the *i*th species and the measured total carbon mass, and the product of this ratio and EF_C was defined as the emission factor of the *i*th species.

[7] Line 232: "NMHCs" should be "speciated NMHCs". In this study, the total NMHCs were not determined. Only a portion of them was speciated.

Response: We have changed "NMHCs" to "speciated NMHCs" in the whole manuscript.

[8] Line 243: I suppose that the particle size evolves through the course of photo-oxidation experiments. Discussion is needed about whether the particle loss during the experiments can be corrected for using post measurements.

Response: We agree that the particle wall loss rate is size-dependent. The relationship between the particle loss rate and the diameter was shown in Figure 1. From burn 1-6, the uncorrected particle size grew from 68 to 92, 71 to 148, 57 to 91, 61 to 98, 82 to 150 and 57 to 105 nm during the photo-oxidation. Assuming that the wall loss rates during the whole photoreaction should correspond to the averaged size of the primary particles and the aged particles, they were underestimated by 5.4%, -2.0%, 8.8%, 7.3%, -2.8% and 7.8%, respectively, when we use the wall loss rates after lights were off for simplification. So it might be acceptable to use post measurements to determine the particle wall loss rate, though an error range of ~±9% should be noted. The discussion above have been added to the supplement material of this manuscript.

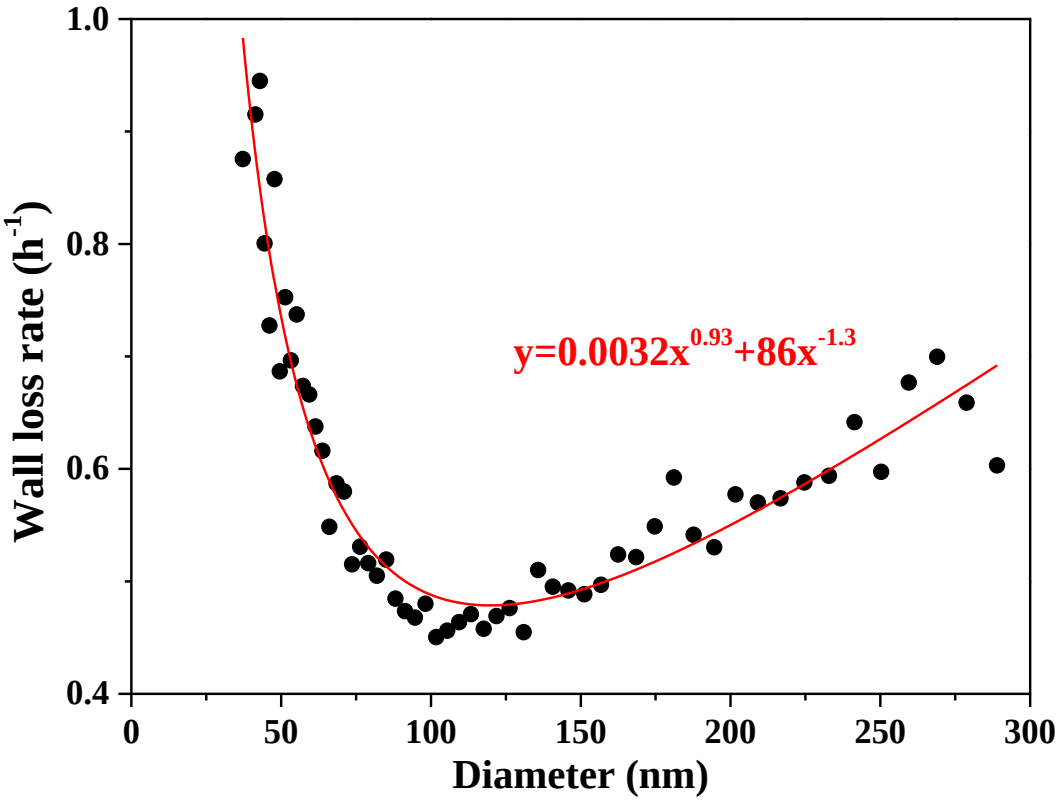

Fig 1. The relationship between wall loss rate and the particle diameter. The data were calculated from burn 6 in which wheat straws were burned. The fitting was based on the equation suggested by Takekawa et al. (2003).

[9] Line 283: NMHCs were measured by two instruments: PTR-MS and GC-MS. Efforts are need to make sure readers can tell these measurements and follow the discussion.

Response: We have added the following statement to Sect 2.2 where PTR-TOF-MS is introduced: "Continuous monitoring of 20 SOA precursors (including 9 NMHCs and 11 oxygen-containing VOCs) from PTR-TOF-MS provided us with data to do the SOA prediction discussed in the Section 2.3.5 and 3.3.2." Also in Sect 2.2 where GC-MSD/FID is introduced, the following sentence has been added: "Results from GC-MSD/FID were used to quantify the emission factors of 67 NMHCs discussed in the Section 3.1."

[10] Line 297: Not all organic vapors were measured in this study. Do authors have an

estimate of the unmeasured vapors across the three fuels and their ozone formation potential?

Response: As replying the referee #2's comment above, some species of NMOGs detected by PTR-TOF-MS are not included in this manuscript for SOA prediction, but they did have both high EFs and high ozone formation potentials. But even with the help of GC-MSD/FID and PTR-TOF-MS, we are not sure to be able to identify and precisely quantify all organic vapors generated from agricultural residues burning because of difficulties in separating isomers from each other (Hatch et al., 2017; Bruns et al., 2017) and because of some intermediate volatility organic compounds are not detected but may also contribute to form SOA and ozone. In fact we are also very interested in this topic and what to know if the "traditional" ozone precursors could explain the ozone formation during our photo-oxidation experiments, and for this we may need to use the MCM model. We have started to write a paper on this aspect. In this manuscript we just put our focus on that if the known precursors could explain the SOA formed during photo-oxidation.

References

Bruns, E. A., El Haddad, I., Slowik, J. G., Kilic, D., Klein, F., Baltensperger, U., and Prevot, A. S. H.: Identification of significant precursor gases of secondary organic aerosols from residential wood combustion, Sci. Rep., 6, doi:10.1038/srep27881, 2016.

Bruns, E. A., Slowik, J. G., El Haddad, I., Kilic, D., Klein, F., Dommen, J., Temime-Roussel, B., Marchand, N., Baltensperger, U., and Prevot, A. S. H.: Characterization of gas-phase organics using proton transfer reaction time-of-flight mass spectrometry: fresh and aged residential wood combustion emissions, Atmos. Chem. Phys., 17, 705-720, doi:10.5194/acp-17-705-2017, 2017.

Carter, W. P. L.: Reactivity estimates for selected consumer product compounds, Air resources Board, California, Contract No. 06-408, 72-99, 2008.

Deng, W., Liu, T., Zhang, Bruns, E. A., El Haddad, I., Slowik, J. G., Kilic, D., Klein, F., Baltensperger, U., and Prevot, A. S. H.: Identification of significant precursor

gases of secondary organic Bruns, E. A., El Haddad, I., Slowik, J. G., Kilic, D., Klein, F., Baltensperger, U., and Prevot, A. S. H.: Identification of significant precursor gases of secondary organic aerosols from residential wood combustion, Sci. Rep., 6, doi:10.1038/srep27881, 2016.

Bruns, E. A., Slowik, J. G., El Haddad, I., Kilic, D., Klein, F., Dommen, J., Temime-Roussel, B., Marchand, N., Baltensperger, U., and Prevot, A. S. H.: Characterization of gas-phase organics using proton transfer reaction time-of-flight mass spectrometry: fresh and aged residential wood combustion emissions, Atmos. Chem. Phys., 17, 705-720, doi:10.5194/acp-17-705-2017, 2017.

Carter, W. P. L.: Reactivity estimates for selected consumer product compounds, Air resources Board, California, Contract No. 06-408, 72-99, 2008. aerosols from residential wood combustion, Sci. Rep., 6, doi:10.1038/srep27881, 2016.

Bruns, E. A., Slowik, J. G., El Haddad, I., Kilic, D., Klein, F., Dommen, J., Temime-Roussel, B., Marchand, N., Baltensperger, U., and Prevot, A. S. H.: Characterization of gas-phase organics using proton transfer reaction time-of-flight mass spectrometry: fresh and aged residential wood combustion emissions, Atmos. Chem. Phys., 17, 705-720, doi:10.5194/acp-17-705-2017, 2017.

Carter, W. P. L.: Reactivity estimates for selected consumer product compounds, Air resources Board, California, Contract No. 06-408, 72-99, 2008.

Y., Situ, S., Hu, Q., He, Q., Zhang, Z., Lü, S., Bi, X., Wang, X., Boreave, A., George, C., Ding, X., and Wang, X.: Secondary organic aerosol formation from photo-oxidation of toluene with NO_x and SO_2: Chamber simulation with purified air versus urban ambient air as matrix, Atmos. Environ., 150, 67-76, doi:10.1016/j.atmosenv.2016.11.047, 2017.

Du, Q., Zhang, C., Mu, Y., Cheng, Y., Zhang, Y., Liu, C., Song, M., Tian, D., Liu, P., Liu, J., Xue, C., and Ye, C.: An important missing source of atmospheric carbonyl sulfide: Domestic coal combustion, Geophys. Res. Lett., 43, 8720-8727, doi:10.1002/2016gl070075, 2016.

Gordon, T. D., Presto, A. A., May, A. A., Nguyen, N. T., Lipsky, E. M., Donahue, N. M., Gutierrez, A., Zhang, M., Maddox, C., Rieger, P., Chattopadhyay, S.,

Maldonado, H., Maricq, M. M., and Robinson, A. L.: Secondary organic aerosol formation exceeds primary particulate matter emissions for light-duty gasoline vehicles, Atmos. Chem. Phys., 14, 4661-4678, doi:10.5194/acp-14-4661-2014, 2014.

Hatch, L. E., Yokelson, R. J., Stockwell, C. E., Veres, P. R., Simpson, I. J., Blake, D. R., Orlando, J. J., and Barsanti, K. C.: Multi-instrument comparison and compilation of non-methane organic gas emissions from biomass burning and implications for smoke-derived secondary organic aerosol precursors, Atmos. Chem. Phys., 17, 1471-1489, doi:10.5194/acp-17-1471-2017, 2017.

Hennigan, C. J., Sullivan, A. P., Collett, J. L., Jr., and Robinson, A. L.: Levoglucosan stability in biomass burning particles exposed to hydroxyl radicals, Geophys. Res. Lett., 37, doi:10.1029/2010gl043088, 2010.

Li, J., Bo, Y., and Xie, S. D.: Estimating emissions from crop residue open burning in China based on statistics and MODIS fire products, J. Environ. Sci., 44, 158-170, doi:10.1016/j.jes.2015.08.024, 2016.

Li, Q., Li, X. H., Jiang, J. K., Duan, L., Ge, S., Zhang, Q., Deng, J. G., Wang, S. X., and Hao, J. M.: Semi-coke briquettes: towards reducing emissions of primary $PM_{2.5}$, particulate carbon, and carbon monoxide from household coal combustion in China, Sci. Rep., 6, 10, doi:10.1038/srep19306, 2016.

Li, X. H., Wang, S. X., Duan, L., and Hao, J. M.: Characterization of non-methane hydrocarbons emitted from open burning of wheat straw and corn stover in China, Environ. Res. Lett., 4, 7, doi:10.1088/1748-9326/4/4/044015, 2009.

Liao, C. P., Wu, C. Z., Yanyongjie, and Huang, H. T.: Chemical elemental characteristics of biomass fuels in China, Biomass Bioenergy, 27, 119-130, doi:f10.1016/j.biombioe.2004.01.002, 2004.

Liu, C., Zhang, C., Mu, Y., Liu, J., and Zhang, Y.: Emission of volatile organic compounds from domestic coal stove with the actual alternation of flaming and smoldering combustion processes, Environ. Pollut., 221, 385-391, doi:10.1016/j.envpol.2016.11.089, 2017.

Liu, J., Mauzerall, D. L., Chen, Q., Zhang, Q., Song, Y., Peng, W., Klimont, Z., Qiu, X.,

Zhang, S., Hu, M., Lin, W., Smith, K. R., and Zhu, T.: Air pollutant emissions from Chinese households: A major and underappreciated ambient pollution source, Proc. Natl. Acad. Sci., doi:10.1073/pnas.1604537113, 2016.

Liu, P. S. K., Deng, R., Smith, K. A., Williams, L. R., Jayne, J. T., Canagaratna, M. R., Moore, K., Onasch, T. B., Worsnop, D. R., and Deshler, T.: Transmission efficiency of an aerodynamic focusing lens system: Comparison of model calculations and laboratory measurements for the Aerodyne Aerosol Mass Spectrometer, Aerosol Sci. Technol., 41, 721-733, doi:10.1080/02786820701422278, 2007.

National bureau of statistics of people's republic of China.: China Energy Statistical Yearbook 2013, China Stat. Press, Beijing, 2014.

Pan, X., Kanaya, Y., Tanimoto, H., Inomata, S., Wang, Z., Kudo, S., and Uno, I.: Examining the major contributors of ozone pollution in a rural area of the Yangtze River Delta region during harvest season, Atmos. Chem. Phys., 15, 6101-6111, doi:10.5194/acp-15-6101-2015, 2015.

Presto, A. A., Miracolo, M. A., Kroll, J. H., Worsnop, D. R., Robinson, A. L., and Donahue, N. M.: Intermediate-volatility organic compounds: A potential source of ambient oxidized organic aerosol, Environ. Sci. Technol., 43, 4744-4749, doi:10.1021/es803219q, 2009.

Takekawa, H., Minoura, H., and Yamazaki, S.: Temperature dependence of secondary organic aerosol formation by photo-oxidation of hydrocarbons, Atmos. Environ., 37, 3413-3424, doi:10.1016/s1352-2310(03)00359-5, 2003.

Tiitta, P., Leskinen, A., Hao, L., Yli-Pirila, P., Kortelainen, M., Grigonyte, J., Tissari, J., Lamberg, H., Hartikainen, A., Kuuspalo, K., Kortelainen, A.-M., Virtanen, A., Lehtinen, K. E. J., Komppula, M., Pieber, S., Prevot, A. S. H., Onasch, T. B., Worsnop, D. R., Czech, H., Zimmermann, R., Jokiniemi, J., and Sippula, O.: Transformation of logwood combustion emissions in a smog chamber: formation of secondary organic aerosol and changes in the primary organic aerosol upon daytime and nighttime aging, Atmos. Chem. Phys., 16, 13251-13269, doi:10.5194/acp-16-13251-2016, 2016.

Tkacik, D. S., Robinson, E. S., Ahern, A., Saleh, R., Stockwell, C., Veres, P., Simpson, I. J., Meinardi, S., Blake, D. R., Yokelson, R. J., Presto, A. A., Sullivan, R. C., Donahue, N. M., and Robinson, A. L.: A dual-chamber method for quantifying the effects of atmospheric perturbations on secondary organic aerosol formation from biomass burning emissions, J. Geophys. Res.-Atmos., 122, 6043-6058, doi:10.1002/2016JD025784, 2017.

Wang, H., Lou, S., Huang, C., Qiao, L., Tang, X., Chen, C., Zeng, L., Wang, Q., Zhou, M., Lu, S., and Yu, X.: Source profiles of volatile organic compounds from biomass burning in Yangtze River Delta, China, Aerosol Air Qual. Res., 14, 818-828, doi:10.4209/aaqr.2013.05.0174, 2014.

Zhao, Y. L., Hennigan, C. J., May, A. A., Tkacik, D. S., de Gouw, J. A., Gilman, J. B., Kuster, W. C., Borbon, A., and Robinson, A. L.: Intermediate-volatility organic compounds: A large source of secondary organic aerosol, Environ. Sci. Technol., 48, 13743-13750, doi:10.1021/es5035188, 2014.

Zhu, Y. H., Yang, L. X., Chen, J. M., Wang, X. F., Xue, L. K., Sui, X., Wen, L., Xu, C. H., Yao, L., Zhang, J. M., Shao, M., Lu, S. H., and Wang, W. X.: Characteristics of ambient volatile organic compounds and the influence of biomass burning at a rural site in Northern China during summer 2013, Atmos. Environ., 124, 156-165, doi:10.1016/j.atmosenv.2015.08.097, 2016.

Open burning of rice, corn and wheat straws: primary emissions, photochemical aging, and secondary organic aerosol formation

Zheng Fang[1,3], Wei Deng[1,3], Yanli Zhang[1,2], Xiang Ding[1], Mingjin Tang[1], Tengyu Liu[1], Qihou Hu[1], Ming Zhu[1,3], Zhaoyi Wang[1,3], Weiqiang Yang[1,3], Zhonghui Huang[1,3], Wei Song[1,2], Xinhui Bi[1], Jianmin Chen[4], Yele Sun[5], Christian George[6], Xinming Wang[1,2,*]

[1]State Key Laboratory of Organic Geochemistry and Guangdong Key Laboratory of Environment Protection and Resources Utilization, Guangzhou Institute of Geochemistry, Chinese Academy of Sciences, Guangzhou 510640, China

[2]Center for Excellence in Regional Atmospheric Environment, Institute of Urban Environment, Chinese Academy of Sciences, Xiamen 361021, China

[3]University of Chinese Academy of Sciences, Beijing 100049, China

[4]Shanghai Key Laboratory of Atmospheric Particle Pollution and Prevention, Department of Environmental Science & Engineering, Fudan University, Shanghai 200433, China

[5]Institute of Atmospheric Physics, Chinese Academy of Sciences, Beijing 100029, China

[6]Institut de Recherches sur la Catalyse et l'Environment de Lyon (IRCELYON), CNRS, UMR5256, Villeurbanne F-69626, France

Correspondence to: X. Wang (wangxm@gig.ac.cn)

Abstract. Agricultural residues are among the most abundant biomass burned globally, especially in China. However, there is rare information on primary emissions and photochemical evolution of agricultural residues burning. In this study, indoor chamber experiments were conducted to investigate primary emissions from open burning of rice, corn and wheat straws and their photochemical aging as well. Emission factors of NO_x, NH_3, SO_2, 67 non-methane hydrocarbons (NMHCs), particulate matter (PM), organic aerosol (OA) and black carbon (BC) under ambient dilution conditions were determined. Olefins accounted for >50% of the total speciated NMHCs emission (2.47 to 5.04 g kg^{-1}), indicating high ozone formation potential of straw burning emissions. Emission factors of PM (3.73 to 6.36 g kg^{-1}) and primary organic carbon (POC, 2.05 to 4.11 gC kg^{-1}), measured at dilution ratios of 1300 to 4000, were lower than those reported in previous studies at low dilution ratios, probably due to the evaporation of semi-volatile organic compounds under high dilution conditions. After photochemical aging with OH exposure range of (1.97-4.97)×10^{10} molecule cm^{-3} s in the chamber, large amounts of secondary organic aerosol (SOA) were produced with OA mass enhancement ratios (the mass ratio of total OA to primary OA) of 2.4-7.6. The 20 known precursors could only explain 5.0-27.3% of the observed SOA mass, suggesting that the major precursors of SOA formed from open straw burning remain unidentified. Aerosol mass spectrometry (AMS) signaled that the aged OA contained less hydrocarbons but more oxygen- and nitrogen-containing compounds than primary OA, and carbon oxidation state (OS_c) calculated with AMS resolved O/C and H/C ratios increased linearly (p<0.001) with OH exposure with quite similar slopes.

1 Introduction

On the global scale, biomass burning (BB) is the main source of primary organic carbon (OC) (Bond et al., 2004; Huang et al., 2015), black carbon (BC) (Bond et al., 2013; Cheng et al., 2016), and brown carbon (BrC) (Laskin et al., 2015). It is also the second largest source of non-methane organic gases (NMOGs) in the atmosphere (Yokelson et al., 2008; Stockwell et al., 2014). In addition, atmospheric aging of biomass burning plumes produces substantial secondary pollutants. The increase of tropospheric ozone (O_3) in aged biomass burning plumes could last for days and even months (Thompson et al., 2001; Duncan et al., 2003; Real et al., 2007) with complex atmospheric chemistry (Arnold et al., 2015; Müller et al., 2016). Moreover, biomass and biofuel burning could contribute up to 70% of global secondary organic aerosols (SOA) burden (Shrivastava et al., 2015) and hence influence the seasonal variation of global SOA (Tsigaridis et al., 2014). Since it produces large amounts of primary and secondary pollutants, it is essential to characterize primary emissions and photochemical evolution of biomass burning in order to better understand its impacts on air quality (Huang et al., 2014), human health (Alves et al., 2015) and climate change (Andreae et al., 2004; Koren et al., 2004; Laskin et al., 2015; Huang et al., 2016).

Open burning of agricultural residues, a convenient and inexpensive way to prepare for the next crop planting, could induce severe regional haze events (Cheng et al., 2013; Tariq et al., 2016). Among all the biomass burning types, agricultural residues burning in the field is estimated to contribute ~10% of the total mass burned globally (Andreae and Merlet, 2001), and its relative contribution is even larger in Asia (~34%) and especially in China (>60%) (Streets et al., 2003) where >600 million people live in the countryside (NBSPRC, 2015). Agricultural residues burned in China were estimated to be up to 160 million tons in 2012, accounting for ~40% of the global agricultural residues burned (Li et al., 2016). As estimated by Tian et al. (2011), agricultural residues burning contributed to 70-80% of non-methane

hydrocarbons (NMHCs) and particulate matter (PM) emitted by biomass burning in China during 2000-2007. A better understanding of the role agricultural residual burning plays in air pollution in China and elsewhere requires better characterization of primary emission and atmospheric aging of emitted trace gases and particles for different types of agricultural residues under different burning conditions.

In the pasted two decades, there have been increasing numbers of characterization of biomass burning emissions. Andreae and Merlet (2001) summarized emission factors (EFs) for both gaseous and particulate compounds from seven types of biomass burning. Akagi et al. (2011) updated the emission data for fourteen types of biomass burning, and newly identified species were included. Since biomass types and combustion conditions may differ in different studies, reported emission factors are highly variable, especially for agricultural residues burning (Li et al., 2007; Cao et al., 2008; Zhang et al., 2008; Li et al., 2009; Yokelson et al., 2011; Brassard et al., 2014; Sanchis et al., 2014; Wang et al., 2014; Ni et al., 2015; Kim Oanh et al., 2015; Stockwell et al., 2016; Bruns et al., 2017; Li et al., 2017; Thacik et al., 2017). Moreover, previous studies on agricultural residues burning were mostly carried out near fire spots or in chambers with low dilution ratios. Since biomass burning organic aerosols (BBOA) are typically semi-volatile (Grieshop et al., 2009b; May et al., 2013), it is expected that measured BBOA emission factors would be affected by dilution processes (Lipsky et al., 2006), and BBOA emission factors under ambient dilution conditions are still unclear. Furthermore, knowledge in NMOGs emitted from agricultural residues burning is very limited. As reported by Stockwell et al. (2015), ~21% (in weight) of NMOGs in biomass burning plumes have not been identified yet. Therefore, comprehensive measurement and characterization of gaseous and particulate species emitted by agricultural residues burning under ambient dilution conditions are urgently needed.

Great attention has been drawn to SOA formation and transformation in biomass burning

plumes recently, since significant increase of mass and apparent change in physicochemical characteristics of aerosols have been observed during atmospheric aging of biomass burning plumes in both field and laboratory studies (Grieshop et al., 2009a,b; Hennigan et al., 2011; Heringa et al., 2011; Lambe et al., 2011; Jolleys et al., 2012; Giordano et al., 2013; Martin et al., 2013; Ortega et al., 2013; Ding et al., 2016a; Ding et al., 2016b; Ding et al., 2017). For agricultural residues burning, evolution processes have not been well characterized yet. To our knowledge, up to now there is only a chamber study (Li et al., 2015) which has investigated the evolution of aerosol particles emitted by wheat straw burning under dark conditions. Although field studies (Adler et al., 2011; Liu et al., 2016) witnessed the evolution in mass concentrations, size distribution, oxidation state and optical properties of aerosol particles emitted by agricultural residues burning, these changes could be also influenced by other emission sources and meteorological conditions as well. Since NMOGs emitted by agricultural residues burning are not fully quantified, it is still challenging to predict the concentration and physicochemical properties of SOA resulted from biomass burning (Spracklen et al., 2011; Jathar et al., 2014; Shrivastava et al., 2015; Hatch et al., 2017). Bruns et al. (2016) suggsted that the 22 major NMOGs identified in residential wood combustion could explain the majority of observed SOA, but it remains unclear whether identified NMOGs emitted by agricultural residues burning could fully (or at least largely) explain the SOA formed. In addition, aerosol mass spectrometry (AMS) has been widely used to characterize sources and evolution of ambient OA (Zhang et al., 2011). Although agricultural residues burning is an important type of biomass burning in Asia and especially in China, the lack of AMS spectra for primary and aged OA from agricultural residues burning significantly limits further application of AMS in BBOA research.

In this study, plumes from agricultural residues open burning were directly introduced into a large indoor chamber to firstly characterize primary emissions and then investigate their

photochemical evolution under ~25°C and ~50% relative humidity. Corn, rice and wheat straws, which accounts for more than 90% of the crop residues burned in China (FAO, 2017), were chosen. A suite of advanced online and offline techniques were utilized to measure gaseous and particulate species, enabling comprehensive measurements of emission factors of gaseous and particulate compounds for burning of each types of straw under ambient dilution conditions. In addition, corresponding formation and transformation of SOA during photochemical aging was investigated using a large indoor smog chamber. This work would help improve our understanding of primary emission, SOA formation and thus environmental impacts of agricultural residues burning.

2 Materials and methods

2.1 Experimental setup

Photochemical aging was investigated in a smog chamber in the Guangzhou Institute of Geochemistry, Chinese Academy of Sciences (GIG-CAS). The GIG-CAS smog chamber is a ~30 m^3 fluorinated ethylene propylene (FEP) reactor housed in a temperature-controlled room. Details of the chamber setup and associated facilities are provided elsewhere (Wang et al., 2014; Liu et al., 2015, 2016; Deng et al., 2017). Briefly, 135 black lamps (1.2 m long, 60 W Philips, Royal Dutch Philips Electronics Ltd, the Netherlands) are used as light sources, giving a NO_2 photolysis rate of approximately 0.25 min^{-1}. Two Teflon-coated fans are installed inside the reactor to ensure introduced gaseous and particulate species mixed well within 2 min. Prior to each experiment, the reactor was flushed with the purified dry air at a rate of 100 L min^{-1} for at least 48 h. The compressed indoor air is forced through an air dryer (FXe1; Atlas Copco; Sweden) and a series of gas scrubbers containing activated carbon, Purafil, Hopcalite and allochroic silica gel, followed by a PTFE filter to provide the source of the purified air. The purified dry air contains <1 ppb NO_x, O_3 and carbonyl compounds, <5 ppb NMHCs and no detectable particles with relative humidity <5%.

Corn, rice and wheat straws were collected from Henan, Hunan and Guangdong province, respectively. Since moisture content in straws would affect emission factors of atmospheric pollutants (Sanchis et al., 2014; Ni et al., 2015), all the agricultural residues used in this study were dried in a stove at 80 °C for 24 h before being burned. After baking, water content in the crop residues was less than 1%. The water content of crop residues was measured by using the method recommended by Liao et al. (2004). The weight of straws were weighed before and after baking in a stove at 105℃ for 24 h, and the difference in weights was calculated to be the weight of the water in the crop residues. Water content was the quotient of the water weight and the whole weight of the straws. In each experiment, ~300 g straws were burned and the burning typically lasted for 3-5 min. Straws were ignited by a butane-fueled lighter and burned under open field burning conditions. The resulting smoke was collected by an inverted funnel and introduced into the chamber using an oil-free pump (Gast Manufacturing, Inc, USA) at a flow rate of ~15 L min^{-1} through a 5.5 m long copper tube (inner diameter: 3/8 inch), and the residence time in the tube was estimated to be <2 s. Before each experiment, the transfer tube was pre-flushed for 15 min with ambient air and 2 min with smokes (not introduced into the chamber reactor). During the whole process, the tube was heated at 80 °C to reduce the losses of organic vapors. Based on the volumes of the smoke introduced and the chamber reactor, the dilution ratios were estimated to be 1300-4000, falling into the typical range (1000-10000) under ambient dilution conditions (Robinson et al., 2007). After being characterized in dark for >20 min, black ~~lumps~~ lamps were turned on and the dilute~~d~~ smoke were photochemically aged for 5 h. At the end, black lamps were switched off and the aged aerosols were characterized in the next one hour to ~~correct~~ determine the particle wall loss. The particle size evolved through the course of photo-oxidation, and the differences in particle wall loss rates during photoreaction and after the lamps were off brought about by the size evolving are estimated to be within ±9% (Figure S1).

In total 20 experiments were conducted (9 for rice straw, 6 for corn straw and 5 for wheat straw), among which 14 experiments were conducted only in the dark to measure primary emissions and 6 experiments were carried out both in the dark and under irradiation to investigate photochemical evolution of open straw burning emissions. Tables 1 and 2 summarize important experimental conditions and key results for all the experiments.

2.2 Instrumentation

~~Gaseous and particulate species were monitored with a suite of online and offline instruments.~~ Commercial instruments were used for online monitoring of NO_x (EC9841T, Ecotech, Australia), NH_3 (Model 911-0016, Los Gatos Research, USA) and SO_2 (Model 43i, Thermo Scientific, USA). CH_4 and CO were analyzed offline using a gas chromatography (Agilent 6980GC, USA) coupled with a flame ionization detector and a packed column (5A molecular sieve 60/80 mesh, 3 m × 1/8 in) (Zhang et al., 2012), and CO_2 was analyzed using a HP 4890D gas chromatograph (Yi et al., 2007). The detection limits were all less than 30 ppbv for CH_4, CO and CO_2. The relative standard deviations (RSDs) of CO and CO_2 measurements were both less than 3% based on seven duplicate injection of 1.0 ppmv standards (Spectra Gases Inc, USA).

Volatile organic compounds (VOCs) were continuously measured using a proton-transfer-reaction time-of-flight mass spectrometer (PTR-TOF-MS; Model 2000, Ionicon Analytik GmbH, Austria). Calibration of the PTR-TOF-MS was performed every few weeks using a certified custom-made standard mixture of VOCs (Ionicon Analytik Gmbh, Austria) that were dynamically diluted to 6 levels (2, 5, 10, 20, 50 and 100 ppbv). Methanol, acetonitrile, acetaldehyde, acrolein, acetone, isoprene, crotonaldehyde, 2-butanone, benzene, toluene, o-xylene, chlorobenzene and α-pinene were included in the calibration mixture. Their sensitivities, indicated by the ratio of the normalized counts per second to the concentration levels of the VOCs in ppbv, were used to convert the raw PTR-TOF-MS signal to concentration

(Huang et al., 2016). Quantification of the compounds that were not included in the mixture was performed by using calculated mass-dependent sensitivities based on the measured sensitivities (Stockwell et al., 2015). Mass-dependent sensitivities were linearly fitted for oxygen-containing compounds and the remaining compounds separately. The decay of toluene measured by PTR-TOF-MS was used to derive the OH radical concentrations for every 2 min during each experiment, and the OH exposure was calculated as the product of the OH concentration and the time interval. Continuous monitoring of 20 SOA precursors (including 9 NMHCs and 11 oxygen-containing VOCs) from PTR-TOF-MS provided us with data to do the SOA prediction discussed in the Sect 2.3.5 and 3.3.2. Air samples were also collected from the chamber reactor using 2-Liter electro-polished stainless-steel canisters before and after smoke injection. In total 67 C_2-C_{12} NMHCs were measured (Table S1) using an Agilent 5973N gas chromatography mass-selective detector/flame ionization detector (GC-MSD/FID; Agilent Technologies, USA) coupled to a Preconcentrator (Model 7100, Entech Instruments Inc., USA), and analytical procedures have been detailed elsewhere (Wang and Wu, 2008; Zhang et al., 2010; Zhang et al., 2012). Results from GC-MSD/FID were used to quantify the emission factors of 67 NMHCs discussed in the Sect 3.1. ~~CH_4 and CO were analyzed using a gas chromatography (Agilent 6980GC, USA) coupled with a flame ionization detector and a packed column (5A molecular sieve 60/80 mesh, 3 m × 1/8 in) (Zhang et al., 2012), and CO_2 was analyzed using a HP 4890D gas chromatograph (Yi et al., 2007). The detection limits were all less than 30 ppbv for CH_4, CO and CO_2. The relative standard deviations (RSDs) of CO and CO_2 measurements were both less than 3% based on seven duplicate injection of 1.0 ppmv standards (Spectra Gases Inc, USA).~~

Particle number/volume concentrations and size distribution were measured with a scanning mobility particle sizer (SMPS; Classifier model 3080, CPC model 3775, TSI Incorporated, USA). The SMPS was operated with a sheath flow of 3.0 L min^{-1} and a sampling

flow of 0.3 L min^{-1}, allowing for a size scanning range of 14 to 760 nm within 255 s. A high-resolution time-of-flight aerosol mass spectrometer (HR-TOF-AMS; Aerodyne Research Incorporated, USA) was used to measure chemical compositions of non-refractory aerosols ~~particles~~ (DeCarlo et al., 2006). The ~~instrument alternated~~HR-ToF-AMS was operated by alternating every ~~one~~ other min between the high sensitivity V mode and the high resolution W mode. The toolkit Squirrel 1.57I was used to obtain real-time concentration variations of sulfate, nitrate, ammonium, chloride and organics, and the toolkit Pika 1.16I was used to determine the detailed compositions of OA (Aiken et al., 2007~~; Aiken et al.~~, 2008; Canagaratna et al., 2015). The AMS signal at m/z 44 was corrected for the contribution from gaseous CO_2. The i~~I~~onization efficiency of the AMS was calibrated routinely by measuring 300 nm monodisperse ammonium nitrate aerosols. Considering the underestimation of particulate matter by the AMS, aerosol mass measured by AMS was corrected with the data from the SMPS and the aethalometer. Conductive silicon tubes were used for aerosol sampling to reduce electrostatic losses of particles.

BC was measured with a seven-channel aethalometer (Model AE-31, Magee Scientific, USA). Cheng et al. (2016) measured the mass absorption efficiency (MAE) of BC from biomass burning at wavelengths of 532 and 1047 nm respectively, and the absorption Ängström exponents (AAE) were estimated to be in the range of 0.9-1.1. Based on relationship between MAE and wavelength, a MAE value of 4.7 m^2 g^{-1} was calculated for 880 nm by assuming the AAE to be 1.0. The MAE value was then applied to convert absorption data in 880 nm to BC mass concentrations. Aethalometer attenuation measurements were corrected for particle loading effects and the scattering of filter fibers using the method developed by Kirchstetter and Novakov (2007) and Schmid et al. (2006).

2.3 Data analysis

2.3.1 Particle effective density

Assuming that particles are spherical and non-porous, the effective density (ρ_{eff}) can be estimated by Eq. (1) (DeCarlo et al. 2004; Schmid et al. 2007):

$$\rho_{eff}=\rho_0 \cdot \frac{d_{va}}{d_m} \quad (1)$$

where ρ_0 is the standard density (1.0 g cm^{-3}), and d_{va} and d_m are the AMS-measured vacuum aerodynamic diameter and SMPS-measured mobility diameter. The input diameters to this equation were determined by comparing distributions of vacuum aerodynamic and electric mobility diameters, using the AMS and SMPS respectively. Derived ρ_{eff} was used to convert volume concentrations of aerosol particles measured by the SMPS to mass concentrations.

2.3.2 Emission factors and modified combustion efficiency

The carbon mass balance approach (Ward et al., 1992; Andreae and Merlet, 2001) was used to calculate fuel based emission factors (EF) for each compound (g kg^{-1} dry fuel). The emission factor for the *i*th species, EF_i, is calculated by Eq. (2):

$$EF_i=\frac{m_i \cdot EF_C}{\Delta[CO_2]+\Delta[CO]+\Delta[PM_C]+\Delta[HC]} \quad (2)$$

where m_i is the concentration (g m^{-3}) of the *i*th species; $\Delta[CO_2]$, $\Delta[CO]$, and $\Delta[HC]$ are the background-corrected carbon mass concentration (g-C m^{-3}) of the CO_2, CO, and speciated hydrocarbons, respectively; $\Delta[PM_C]$ is the background-corrected carbon in the particle phase (g-C m^{-3}); EF_C is the emission factor of carbon into the air determined by elemental and gravitational ~~analysis~~analyses, given by Eq. (3):

$$EF_C=\frac{m_{fuel} \cdot \omega_{fuel}-m_{ash} \cdot \omega_{ash}}{m_{fuel}} \quad (3)$$

where ω_{fuel} and ω_{ash} are mass fractions of carbon in the dry fuel and its ash, and m_{fuel} and m_{ash} are the mass of dry fuel and its ash. The modified combustion efficiency (MCE) is defined by Eq. (4) (Heringa et al., 2011; Hennigan et al., 2011; Ni et al., 2015):

$$MCE=\frac{\Delta[CO_2]}{\Delta[CO_2]+\Delta[CO]} \quad (4)$$

2.3.3 Ozone formation potential

The ozone formation potential (OFP) of the speciated NMHCs was calculated from the emission factor and maximum incremental reactivity (MIR) of each individual NMHCs, using Eq. (5):

$$OFP=\sum_{i=1}^{n}(EF_i \cdot MIR_i) \quad (5)$$

where OFP is the ozone formation potential of NMHCs emitted from per unit of biomass (unit: g kg^{-1}), and MIR_i is the MIR of the *i*th NMHC (unit: g O_3 per g NMHC) (Carter, 2008).

2.3.4 Wall loss corrections

Due to the loss of particles and vapors to chamber walls, measured data in chamber studies need to be corrected for wall loss. For this purpose, in our study one-hour dark decay of aged aerosols was undertaken after photochemical aging was terminated. The loss of particles on the chamber wall is a first-order process (McMurry and Grosjean, 1985). The wall-loss rates of AMS-measured organics, sulfate, nitrate, chloride and ammonium were determined using the dark decay data and were applied to wall-loss correction for the entire experiment. By assuming that the condensed materials on the wall remains completely in equilibrium with the gas phase, we used the ω=1 case to correct the OA mass, where ω is a proportionality factor of organic vapor partitioning to chamber walls and suspended particles (Weitkamp et al., 2007; Henry et al., 2012). For SMPS measurements, the number concentration in each size channel (110 channels in total) was corrected for wall loss separately, since wall loss rates of aerosol particles are size-dependent (Takekawa et al., 2003).

2.3.5 OA production prediction

In this study, twenty NMOGs which have been used to estimate SOA yields by previous work (Ng et al., 2007b; Chan et al., 2009; Hildebrandt et al., 2009; Gómez Alvarez et al., 2009; Chan et al., 2010; Shakya and Griffin, 2010; Chhabra et al., 2011; Nakao et al., 2011; Borras and

Tortajada-Genaro, 2012; Yee et al., 2013; Lim et al., 2013) were ~~identified~~ quantified using PTR-TOF-MS, and the applied SOA yields are summarized in Table S2. The mass concentration of SOA ($[SOA]_{predicted}$, μg m^{-3}) formed from these twenty precursors can be estimated using Eq. (6):

$$[SOA]_{predicted} = \sum_i (\Delta[X_i] \cdot Y_i) \qquad (6)$$

where $\Delta[X_i]$ (μg m^{-3}) is the reacted amount of the *i*th gas-phase precursor and Y_i is the corresponding SOA yield.

Assuming that primary OA (POA) levels kept constant during aging processes, the mass concentration of SOA formed could be estimated as the difference in OA mass concentrations before and after photochemical aging. It should be noted that POA would decrease during aging processes (Tiitta et al., 2016), probably leading to the underestimation of the formed SOA. In papers where those SOA yields were borrowed from, no organic vapor wall loss were accounted for when calculating the mass concentration of the formed SOA, so the same wall loss correction method was used when comparing the predicted SOA and the formed SOA.

3 Results and discussion

3.1 Emissions of gaseous pollutants

Table 1 compares emission factors of gaseous and particulate species measured in our and previous studies. In our study, emission factors of NO_x were 1.47±0.61, 5.00±3.94, and 3.08±0.93 g kg^{-1} for rice, corn and wheat straw, and NO accounted for 84±11% of NO_x primary emission for all experiments. Emission factors of NH_3 were measured to be 0.45±0.15, 0.63±0.30 and 0.22±0.19 g kg^{-1} for rice, corn and wheat straw. Our measured emission factors of reactive nitrogen species were comparable to those reported by previous studies (Li et al. 2007; Tian et al. 2011). Emission factors of SO_2 were 0.07±0.07, 0.99±1.53 and 0.72±0.34 g kg^{-1} for rice, corn and wheat straw. Our measured emission factors of SO_2 were lower than those reported by Cao et al., (2008) and Kim Oanh et al. (2015) for rice straw, but higher than

those reported by Cao et al., (2008) for corn and wheat straw. Due to low sulfur contents in crop straws, the SO_2 emission factors for open burning of crop residues were much lower than those for domestic coal combustion, which were determined to be 2.43-5.36 g kg^{-1} for raw bituminous coal (Du et al., 2016).

Emission factors of the total speciated NMHCs analysed by the GC-MSD/FID system were 5.04±2.04, 2.47±2.11 and 3.08±2.43 g kg^{-1} for rice, corn and wheat straw, respectively (Table 1). Our results were higher than those reported by previous studies (Li et al., 2009; Wang et al., 2014), partly due to the fact that more NMHCs were analyzed in our study (67 species in total). As shown in Figure 1a-c, olefins and acetylene accounted for 56-58% of the total speciated NMHCs, followed by alkanes (22-28%) and aromatic hydrocarbons (16-21%). Table S1 and Figure 2 show the emission factors of each NMHC for open burning of different straws. Emission factors of unsaturated hydrocarbons ranged from 1.37 (corn) to 2.91 g kg^{-1} (rice), with the majority being ethene, acetylene and propene. Emission factors of alkanes ranged from 0.69 (corn) to 1.09 g kg^{-1} (rice), with ethane and propane being the two most abundant compounds. The emission factors of aromatic hydrocarbons were in the range of 0.42 (corn) to 1.04 (rice), and benzene and toluene are dominant species. It is worth noting that major compounds in the three groups (alkanes, alkenes and aromatic hydrocarbons) were all negatively correlated with the modified combustion efficiency (Figure ~~S1~~S2), suggesting that more efficient combustion would reduce their emissions.

Based on their emission factors, we calculated the ozone formation potential for each NMHC. The summed ozone formation potential were 22.5±10.1, 13.7±12.4 and 16.3±13.5 g kg^{-1} for open burning of rice, corn and wheat straw, respectively. As shown in Figure 1d-e, the relative contributions of olefins to the total ozone formation potential could reach >80%. Ethene was the largest ozone precursor (35-42%), followed by propene (16-28%), and these two compounds contributed 58-64% of the total ozone formation potential. Although the

emission factors of aromatic hydrocarbons were lower than those of alkanes, their ozone formation potential was dominant over those of alkanes, with toluene being the largest contributor among all the aromatic hydrocarbons. The contribution of alkanes to the total ozone formation potential was minor (2-3%). It is noted that oxygen-containing organic vapors in agricultural residues burning plumes could also have large ozone formation potentials. For example, the OFPs of formaldehyde and acetaldehyde for all experiments were 0.57-2.46 times of the 67 speciated NMHCs.

3.2 Emission of particulate matters

The emission factors of particulate matters were 3.73±3.28, 5.44±3.43, 6.36±2.98 g kg^{-1} for rice, corn and wheat straw, lower than those reported in the previous studies (Table 1). As suggested by Robinson et al. (2007), the POA emission factors would decrease with increasing dilution ratios, due to evaporation of semi-volatile organic compounds. In this study, the dilution ratios ranged from 1300 to 4000, which were within the typical range of ambient dilution ratios (1000-10000) (Robinson et al. 2007). Therefore, it can be expected that emission factors of primary organic carbon (POC) measured in our study (2.05-4.11 gC kg^{-1}) were lower than those measured by previous work with dilution ratios of 5-20 (Li et al. 2007; Ni et al. 2015). Moreover, it has been shown that the modified combustion efficiency could affect emission factors (Heringa et al., 2011; Stockwell et al., 2015). Figure ~~S2~~ S3 shows negative correlations of the modified combustion efficiency with emission factors of PM and POC (p<0.05 for both cases), indicating that enhancement of combustion efficiency could reduce the emissions of PM and POC. In our study, all straws were pre-baked to reduce the moisture content to <1%, and this treatment could increase the modified combustion efficiency and thus reduce emission factors of particulate matters (Ni et al., 2015). In addition, the amount of straws burned each time in our experiments was much less than that in the fields, which is expected to avoid oxygen deficit during burning to some extent and thus increase the modified

366 combustion efficiency as well.

367 While POA emission factors showed large variability for different types of straw, BC
368 emission factors were relatively constant (0.22-0.27 gC kg^{-1}). Since BC is a mixture of non-
369 volatile compounds in particulate matters, as expected, its emission factors measured in our
370 work were comparable to those reported under lower dilution conditions (Li et al. 2007; Ni et
371 al. 2015). The Δ[POA]/Δ[CO] ratios ranged from 0.022 to 0.133 in our study, larger than those
372 (0.001-0.067) measured in chamber studies for hard- and soft-wood fires (Grieshop et al.,
373 2009b) and vegetation commonly burned in North American wildfires (Heringa et al., 2011),
374 but lower than those (0.051-0.329) obtained in field campaigns (Jolleys et al., 2012).

375 For particle numbers, the emission factors were $(2.94\pm0.91)\times10^{15}$, $(7.29\pm4.17)\times10^{15}$,
376 $(5.87\pm2.89)\times10^{15}$ particle kg^{-1} for rice, corn and wheat straw, respectively (Table 1). Our results
377 were comparable to that (1×10^{15} particle kg^{-1}) for crop residues burning (Andreae and Merlet,
378 2001) and those (3.2×10^{15}-10.9×10^{15} particle kg^{-1}) for wood burning (Hosseini et al., 2013) but
379 two magnitudes larger than those for crop residues burning in a sealed stove (Zhang et al. 2008).

380 **3.3 Evolution of particles**

381 **3.3.1 Growth of particle size**

382 Figure 3 shows the evolution of particle size distribution after photochemical aging of 0, 0.5,
383 2.5 and 5 h. Aerosol particles emitted from open straw burning were peaked at ~~40~~50 ~~-80~~ 90 nm
384 under ambient dilution conditions. The geometric mean diameters for primarily emitted
385 particles in this study were smaller than those (100-150 nm) reported for crop residuals burning
386 under low dilution conditions (Zhang et al., 2011; Li et al., 2015), probabley due to evaporation
387 of organic vapors under the high dilution conditions (Lipsky et al., 2006) and coagulation of
388 fine particles under the low dilution conditions (Hossain et al., 2012).

389 After switching on black lamps, apparent growth of particle size was observed. In all the
390 aging experiments, growth rates of particle diameters in the first 0.5 h were 10 times larger

than those afterwards, and after 5 h aging the geometric mean diameters peaked at 60-120 nm. For instance, in the photochemical aging experiment for wheat straw burning (Figure 3c), the growth rate of particles was 18 nm h^{-1} in the first 0.5 h and decreased to ~1 nm h^{-1} during the following 4.5 h. The size distribution of aged aerosol particles in our study is similar to those of ambient particles under the severe biomass burning impact during haze events (Betha et al., 2014; Niu et al., 2016).

3.3.2 Particle mass enhancement

Figure 4 shows the chemical evolution of aerosol particles during the 5 h photochemical aging of wheat straw burning. During the whole process, OA kept increasing and was dominant over inorganic species. After 3 h of photochemical aging, the levels of all the inorganic species were constant, and nitrate was the second most abundant component with a mass fraction of 7%, followed by chloride (2%), ammonium (1%) and sulfate (<1%). Figure 4b depicts [OA] evolution as a function of OH exposure. OA increased slowly at the first ~0.2 h, and then increased rapidly with OH exposure.

The OA enhancement ratio, defined as the mass ratio of aged OA at the end of each aging experiment to POA, was calculated. In the six aging experiments, the OH exposure and OA enhancement ratios ranged from (1.87-4.97)×10^{10} molecule cm^{-3} s and 2.4-7.6, respectively. Assuming an average OH concentration of 1.5×10^{6} molecule cm^{-3} in the ambient air (Hayes et al., 2013), this means that rapid SOA formation would occur in 3.5-9.2 h during the daytime after straw burning. The OA enhancement ratios determined in our study were higher than those (0.7-2.9) for the combustion of vegetation commonly burned in North American wildfires (Hennigan et al., 2011), and comparable to those (0.7-6.9) for wood burning (Grieshop et al., 2009b; Heringa et al., 2011).

Recently, Bruns et al., (2016) found that 22 NMOGs emitted from residential wood burning could explain the majority of the formed SOA. In our study, 20 of the 22 NMOGs were

detected and quantified with the PTR-TOF-MS. Concentration differences of each compound before and after photo-oxidation were calculated to estimate the SOA formed from these precursors. Since SOA formation highly depends on oxidation conditions, SOA yields for a certain precursor vary with VOC/NO_x ratios. In our work, we chose a set of SOA yields for these NMOGs based on the observed VOC/NO_x ratio in the chamber experiments. More specifically, if the observed VOC/NO_x ratio for a certain precursor in the chamber was within the VOC/NO_x range reported in literature, the mean value of the highest and lowest yields within the VOC/NO_x range in literature was used to estimate the SOA formed from the precursor in the chamber; if the observed VOC/NO_x ratio for a certain precursor was higher than the maximum VOC/NO_x ratio reported in literature, we chose the yield reported at the maximum VOC/NO_x ratio; if the observed VOC/NO_x ratio was lower than the minimum VOC/NO_x ratio reported in literature, we chose the yield reported at the minimum VOC/NO_x ratio.

Figure 5a shows the time series of POA, $SOA_{predicted}$ and unexplained SOA in a typical aging experiment. The contribution of $SOA_{predicted}$ by the 20 NMOGs was minor, and large fractions of observed SOA could not be explained. In all the experiments, only 5.0-27.3% of the observed SOA mass could be explained by the 20 NMOGs (Figure 5b). Even if the highest SOA yield for each precursor reported in literature was used, 60-90% of observed SOA mass still could not be explained. It has been suggested that aqueous-phase oxidation of alkenes could produce substantial SOA (Ervens et al., 2011). Considering large emissions of olefins from straw burning (Figure 1a-c), we also estimated the SOA formed from the three most abundant alkenes (ethene, acetylene, and propene) with their newly-developed SOA yields (Ge et al., 2016; Jia and Xu, 2016; Ge et al., 2017), and their total contribution to the observed SOA was found to be negligible (<0.5%). It is noted that although over 80 VOCs species were quantified by the GC-MSD/FID and the PTR-TOF-MS in this study, only 20 species among

them were taken into the SOA prediction because of the lack of published data for SOA yields. The unaccounted VOC species might be a reason for the discrepancy. On the other hand, as indicated by Deng et al. (2017), SOA yields obtained from chamber studies in purified air matrix might be lower than that in real ambient air matrix. Consequently, using SOA yields from studies in purified air matrix might also under predict SOA yields in the complex biomass burning plume matrix. Moreover, oxidation of particulate organic matters (POM), like semi-volatile organic compounds (SVOC) and intermediate volatility organic compounds (IVOC), would also contribute substantially to SOA formation (Presto et al., 2009; Zhao et al., 2014), yet this is not accounted for in our prediction. ~~Therefore~~Above all, there are still unknown precursors and/or physicochemical processes contributing the majority of SOA formed from open straw burning.

3.3.3 OA mass spectrum evolution

In the high resolution W mode of AMS, ions generated from particles could be identified by their exact mass-charge ratio (m/z) and then grouped into CHON, CHO, CHN and CH families. Figure 6 presents the evolution of OA mass spectra. For POA (Figure 6a), CH-family was the major component with a mass fraction of 68%, followed by CHO (23%), CHN (6%), and CHON (2%). The ions at m/z 43, 41 and 55 were the dominant peaks in the POA mass spectrum. The major ions at m/z 27, 39, 41, 55, 57, 67 and 69 belonged to the CH-family and could be the fragments of hydrocarbons (Weimer et al., 2008). The peaks at m/z 28, 29, 43, 44 and 55 contained considerable CHO ions, and the corresponding ions (CO^+, CHO^+, $C_2H_3O^+$, CO_2^+ and $C_3H_3O^+$) could be the fragments of aldehydes, ketones and carboxylic acid (Ng et al., 2011a). The peak at m/z 91 was mainly attributed to $C_7H_7^+$, possibly originating from aromatic compounds.

The mass spectra of aged OA was quite different from that of POA (Figure 6b-c). The mass fraction of the CH-family decreased to 46% and was comparable to that of CHO-family, while

466 the contribution of N-containing OA (CHN and CHON) increased to ~11%. The ions at m/z 44
467 and 43, mainly coming from the CHO-family, became the dominant peaks for the aged OA.
468 The fractions of two major masses at m/z 44 (f_{44}) and m/z 43 (f_{43}) in OA can be used to generate
469 an f_{44} vs. f_{43} triangular space, in which oxygenated organic aerosol (OOA) moves towards the
470 apex during the aging process (Ng et al., 2010). In addition, f_{44} in the ambient air was suggested
471 to be 0.07±0.04 for semi-volatile OOA (SV-OOA) and 0.17±0.04 for low-volatility OOA (LV-
472 OOA), respectively (Ng et al., 2010). Figure 7a plots f_{44} and f_{43} of the POA and the aged OA
473 in all the six experiments. Most of data are within the f_{44} vs. f_{43} triangular space and close to
474 the left margin. Photochemical aging led to increase in f_{44} for all the experiments, suggesting
475 transformation of OA from SV-OOA to LV-OOA. For comparison, the f_{43} did not change
476 significantly in all the experiments. The main ions at m/z 43 were $C_2H_3O^+$ and $C_3H_7^+$. It can be
477 observed in Figure 6c that the increased contribution of $C_2H_3O^+$ and the decrease contribution
478 of $C_3H_7^+$ were comparable during photoreaction.

479 The ion at m/z 60, mainly consisting of $C_2H_4O_2^+$, is regarded as a BBOA marker, and the
480 mass fraction of this ion in OA, f_{60}, is widely used to probe the evolution of BBOA (Brito et
481 al., 2014; May et al., 2015). Figure 7b plots evolution of f_{44} and f_{60} in all the experiments
482 conducted in this study, in order to compare with measurements in aging biomass burning
483 plumes (Cubison et al., 2011) and those in the POA from different types of biomass burning
484 (Alfarra et al., 2007; Brito et al., 2014; May et al., 2015). Photo-oxidation caused increase in
485 f_{44} and decrease in f_{60}, and this is consistent with the general evolution of OA in ambient
486 biomass burning plumes (Cubison et al., 2011). However, our measured f_{60}, 0.003-0.006 in the
487 POA from open straw burning and 0.002-0004 in aged OA, were all lower than those from
488 other field campaigns and quite near the background f_{60} level of 0.003 for ambient OA (Cubison
489 et al., 2011; Figure 7b). Low values of f_{60} (0.005-0.02) were also reported by Hennigan et al.
490 (2011) in a chamber study for fuels commonly burned in wildfires. In their study, biomass

burning took place in a 3000 m^3 combustion chamber, and the smokes were then injected into another chamber for aging experiments with a dilution ratio of ~25. Previous studies have demonstrated that levoglucosan is a semi-volatile compound with a saturation concentration of ~8 μg m^{-3} at 293 K (Grieshop et al., 2009b; Huffman et al., 2009; Hennigan et al. 2011). As a result, high dilution conditions used in our study would cause levoglucosan to evaporate, and this may at least partly explain the low f_{60} observed in the POA from straw burning. From previous studies, the levoglucosan/OC ratios of straw burning ranging from 4.92 to 16.8% (4 types of vegetation summarized; Dhammapala et al., 2007; Kim Oanh et al., 2011; Hall et al., 2012) were not significantly (two-sample t-test, $p>0.05$) lower than those of prescribed fuel burning, wildfire and wood burning ranging from 1.46 to 13.5% (20 types of vegetation summarized; Hosseini et al., 2013; Shahid et al., 2015). So the difference in fuel type cannot explain the lower f_{60} observed in our study.

3.3.4 Elemental ratio and oxidation state of OA

In this study, the O/C and H/C ratios in the POA from different straws burning were in the range of 0.20-0.38 and 1.58-1.74, respectively. After 5 h aging, O/C increased and H/C decreased (Table 2). Kroll et al. (2011) proposed a metric, the average carbon oxidation state (OS_c), to describe the degree of oxidation of atmospheric organic species. OS_c could be calculated from the elemental composition of OA measured by AMS, given by Eq. (7):

$$OS_c = 2 \times O/C - H/C \qquad (7)$$

In this study, the OS_c values for the fresh POA from open straw burning ranged from -1.25 to -0.89, consistent with those suggested for BBOA (-1 to -0.7) (Kroll et al. 2011). During photochemical aging, the OS_c values increased linearly ($p<0.001$) with OH exposure (Figure 8), and the slopes were quite near each other even for different types of straws, implying AMS measured OS_c might be a good indicator of OH exposure and thereby of photochemical aging.

Figure 9 shows the Van Krevelen diagram of OA. In this study, the slopes of linear

correlations between H/C and O/C range from -0.49 to -0.24 for the five experiments. Slopes of -1, 0.5 and 0 in the Van Krevelen diagrams indicate addition of carboxylic acids without fragmentation, addition of carboxylic acids with fragmentation, and addition of alcohols/peroxides, respectively (Heald et al., 2010; Ng et al., 2011a). Therefore, the slopes determined in our study suggest that open straw burning OA aging resulted in net changes in chemical composition equivalent to addition of carboxylic acid groups with C-C bond breakage and addition of alcohol/peroxide functional groups.

4 Conclusion

In this study, primary emissions of open burning of rice, corn and wheat straw and their photochemical were investigated using a large indoor chamber. Emission factors of NO_x, NH_3, SO_2, 67 NMHCs, PM and particle number were measured under dilution ratios ranging from 1300 to 4000. Emission factors of PM (3.73-6.36 g kg^{-1}) and POC (2.05-4.11 gC kg^{-1}) were lower than those reported in previous studies conducted at lower dilution ratios, probably due to the evaporation of semi-volatile organic compounds. Emission factors of POC, PM and major NMHCs compounds were all negatively correlated with the modified combustion efficiency, suggesting that incomplete burning of agricultural residues could lead to larger primary emission.

Both agricultural residues burning and domestic coal combustion have been recognized to contribute substantially to the deteriorating regional air quality especially in rural areas of China (Pan et al., 2015; Liu et al., 2016; Zhu et al., 2016). The emission factors of the speciated NMHCs, PM, NO_x, CO and SO_2 from combustion of raw bituminous, which is currently prevailing for cooking and heating in rural areas, have been reported to be 0.56-5.40, 25.49±2.30, 0.97±0.03, 208±5 and 2.43-5.36 g kg^{-1}, respectively (Du et al., 2016; Li et al., 2016; Liu et al., 2017). Annually burned crop residues and domestic coals were estimated to be 160 Tg (Li et al., 2016) and 99.6 Tg (NBSPRC, 2014) in China. Therefore, with the emission

factors of the speciated NMHCs (2.47-5.04 g kg^{-1}), PM (3.73-6.36 g kg^{-1}), NO_x (1.47-5.00 g kg^{-1}), CO (46.1-63.5 g kg^{-1}) and SO_2 (0.07-0.99 g kg^{-1}) measured for agricultural residues burning in this study, agricultural residues burning might emit more NMHCs and NO_x, but less primary PM, CO and SO_2 than domestic coal burning on a national scale.

Photochemical aging of primary emissions was investigated with OH exposure equal to 3.2-9.2 hours under typical ambient conditions, and at the end of experiments the OA mass concentrations increased by a factor of 2.4-7.6, suggesting that SOA could be rapidly produced within several hours. Our estimation suggests that phenols are the most important identified SOA precursors, and more than 70% of the formed OA still cannot be explained by the oxidation of known precursors. Measurements using HR-TOF-AMS reveal that after photochemical aging, signals for oxygen- and nitrogen-containing compounds were largely increased, with OS_c increased in a highly significant linear way with OH exposure.

Acknowledgements

This study was supported by Strategic Priority Research Program of the Chinese Academy of Sciences (Grant No. XDB05010200), National Natural Science Foundation of China (Grant No. 41530641/41571130031/41673116/41503105), National Key Research and Development Program (2016YFC0202204) and Guangzhou Science Technology and Innovation Commission (201505231532347).

References

Adler, G., Flores, J. M., Riziq, A. A., Borrmann, S., and Rudich, Y.: Chemical, physical, and optical evolution of biomass burning aerosols: a case study, Atmos. Chem. Phys., 11, 1491-1503, doi:10.5194/acp-11-1491-2011, 2011.

Aiken, A. C., DeCarlo, P. F., and Jimenez, J. L.: Elemental analysis of organic species with

566 electron ionization high-resolution mass spectrometry, Anal. Chem., 79, 8350-8358,
567 doi:10.1021/ac071150w, 2007.
568 Aiken, A. C., Decarlo, P. F., Kroll, J. H., Worsnop, D. R., Huffman, J. A., Docherty, K. S.,
569 Ulbrich, I. M., Mohr, C., Kimmel, J. R., Sueper, D., Sun, Y., Zhang, Q., Trimborn, A.,
570 Northway, M., Ziemann, P. J., Canagaratna, M. R., Onasch, T. B., Alfarra, M. R., Prevot,
571 A. S. H., Dommen, J., Duplissy, J., Metzger, A., Baltensperger, U., and Jimenez, J. L.:
572 O/C and OM/OC ratios of primary, secondary, and ambient organic aerosols with high-
573 resolution time-of-flight aerosol mass spectrometry, Environ. Sci. Technol., 42, 4478-
574 4485, doi:10.1021/es703009q, 2008.
575 Akagi, S. K., Yokelson, R. J., Wiedinmyer, C., Alvarado, M. J., Reid, J. S., Karl, T., Crounse,
576 J. D., and Wennberg, P. O.: Emission factors for open and domestic biomass burning for
577 use in atmospheric models, Atmos. Chem. Phys., 11, 4039-4072, doi:10.5194/acp-11-
578 4039-2011, 2011.
579 Alfarra, M. R., Prevot, A. S. H., Szidat, S., Sandradewi, J., Weimer, S., Lanz, V. A., Schreiber,
580 D., Mohr, M., and Baltensperger, U.: Identification of the mass spectral signature of
581 organic aerosols from wood burning emissions, Environ. Sci. Technol., 41, 5770-5777,
582 doi:10.1021/es062289b, 2007.
583 Alves, N. d. O., Brito, J., Caumo, S., Arana, A., Hacon, S. d. S., Artaxo, P., Hillamo, R., Teinila,
584 K., Batistuzzo de Medeiros, S. R., and Vasconcellos, P. d. C.: Biomass burning in the
585 Amazon region: Aerosol source apportionment and associated health risk assessment,
586 Atmos. Environ., 120, 277-285, doi:10.1016/j.atmosenv.2015.08.059, 2015.
587 Andreae, M. O., and Merlet, P.: Emission of trace gases and aerosols from biomass burning,
588 Global Biogeochem. Cy., 15, 955-966, doi:10.1029/2000GB001382, 2001.
589 Andreae, M. O., Rosenfeld, D., Artaxo, P., Costa, A. A., Frank, G. P., Longo, K. M., and Silva-
590 Dias, M. A. F.: Smoking Rain Clouds over the Amazon, Science, 303, 1337-1342,

591 doi:10.1126/science.1092779, 2004.
592 Arnold, S. R., Emmons, L. K., Monks, S. A., Law, K. S., Ridley, D. A., Turquety, S., Tilmes,
593 S., Thomas, J. L., Bouarar, I., Flemming, J., Huijnen, V., Mao, J., Duncan, B. N., Steenrod,
594 S., Yoshida, Y., Langner, J., and Long, Y.: Biomass burning influence on high-latitude
595 tropospheric ozone and reactive nitrogen in summer 2008: a multi-model analysis based
596 on POLMIP simulations, Atmos. Chem. Phys., 15, 6047-6068, doi:10.5194/acp-15-6047-
597 2015, 2015.
598 Betha, R., Zhang, Z., and Balasubramanian, R.: Influence of trans-boundary biomass burning
599 impacted air masses on submicron particle number concentrations and size distributions,
600 Atmos. Environ., 92, 9-18, doi:10.1016/j.atmosenv.2014.04.002, 2014.
601 Bond, T. C., Doherty, S. J., Fahey, D. W., Forster, P. M., Berntsen, T., DeAngelo, B. J., Flanner,
602 M. G., Ghan, S., Kaercher, B., Koch, D., Kinne, S., Kondo, Y., Quinn, P. K., Sarofim, M.
603 C., Schultz, M. G., Schulz, M., Venkataraman, C., Zhang, H., Zhang, S., Bellouin, N.,
604 Guttikunda, S. K., Hopke, P. K., Jacobson, M. Z., Kaiser, J. W., Klimont, Z., Lohmann,
605 U., Schwarz, J. P., Shindell, D., Storelvmo, T., Warren, S. G., and Zender, C. S.: Bounding
606 the role of black carbon in the climate system: A scientific assessment, J. Geophys. Res.-
607 Atmos., 118, 5380-5552, doi:10.1002/jgrd.50171, 2013.
608 Bond, T. C., Streets, D. G., Yarber, K. F., Nelson, S. M., Woo, J. H., and Klimont, Z.: A
609 technology-based global inventory of black and organic carbon emissions from
610 combustion, J. Geophys. Res.-Atmos., 109, 43, doi:10.1029/2003jd003697, 2004.
611 Borras, E., and Tortajada-Genaro, L. A.: Secondary organic aerosol formation from the photo-
612 oxidation of benzene, Atmos. Environ., 47, 154-163, doi:10.1016/j.atmosenv.2011.11.020,
613 2012.
614 Brassard, P., Palacios, J. H., Godbout, S., Bussieres, D., Lagace, R., Larouche, J. P., and
615 Pelletier, F.: Comparison of the gaseous and particulate matter emissions from the

combustion of agricultural and forest biomasses, Bioresour. Technol., 155, 300-306, doi:10.1016/j.biortech.2013.12.027, 2014.

Brito, J., Rizzo, L. V., Morgan, W. T., Coe, H., Johnson, B., Haywood, J., Longo, K., Freitas, S., Andreae, M. O., and Artaxo, P.: Ground-based aerosol characterization during the South American Biomass Burning Analysis (SAMBBA) field experiment, Atmos. Chem. Phys., 14, 12069-12083, doi:10.5194/acp-14-12069-2014, 2014.

Bruns, E. A., El Haddad, I., Slowik, J. G., Kilic, D., Klein, F., Baltensperger, U., and Prevot, A. S. H.: Identification of significant precursor gases of secondary organic aerosols from residential wood combustion, Sci. Rep., 6, doi:10.1038/srep27881, 2016.

Bruns, E. A., Slowik, J. G., El Haddad, I., Kilic, D., Klein, F., Dommen, J., Temime-Roussel, B., Marchand, N., Baltensperger, U., and Prevot, A. S. H.: Characterization of gas-phase organics using proton transfer reaction time-of-flight mass spectrometry: fresh and aged residential wood combustion emissions, Atmos. Chem. Phys., 17, 705-720, doi:10.5194/acp-17-705-2017, 2017.

Canagaratna, M. R., Jimenez, J. L., Kroll, J. H., Chen, Q., Kessler, S. H., Massoli, P., Hildebrandt Ruiz, L., Fortner, E., Williams, L. R., Wilson, K. R., Surratt, J. D., Donahue, N. M., Jayne, J. T., and Worsnop, D. R.: Elemental ratio measurements of organic compounds using aerosol mass spectrometry: characterization, improved calibration, and implications, Atmos. Chem. Phys., 15, 253-272, doi:10.5194/acp-15-253-2015, 2015.

Cao, G., Zhang, X., Gong, S., and Zheng, F.: Investigation on emission factors of particulate matter and gaseous pollutants from crop residue burning, J. Environ. Sci., 20, 50-55, doi:10.1016/S1001-0742(08)60007-8, 2008.

Carter, W. P. L.: Reactivity estimates for selected co~~m~~nsumer product compounds~~.~~, Air resources Board, Californ̲ia, Contract No. 06-408, 72-99, 2008.

Chan, A. W. H., Kautzman, K. E., Chhabra, P. S., Surratt, J. D., Chan, M. N., Crounse, J. D.,

641 Kürten, A., Wennberg, P. O., Flagan, R. C., and Seinfeld, J. H.: Secondary organic aerosol
642 formation from photooxidation of naphthalene and alkylnaphthalenes: implications for
643 oxidation of intermediate volatility organic compounds (IVOCs), Atmos. Chem. Phys., 9,
644 3049-3060, doi:10.5194/acp-9-3049-2009, 2009.
645 Chan, A. W. H., Chan, M. N., Surratt, J. D., and Chhabra, P. S.: Role of aldehyde chemistry
646 and NO_x concentrations in secondary organic aerosol formation, Atmos. Chem. Phys., 10,
647 7169-7188, doi:10.5194/acp-10-7169-2010, 2010.
648 Cheng, Y., Engling, G., He, K. B., Duan, F. K., Ma, Y. L., Du, Z. Y., Liu, J. M., Zheng, M., and
649 Weber, R. J.: Biomass burning contribution to Beijing aerosol, Atmos. Chem. Phys., 13,
650 7765-7781, doi:10.5194/acp-13-7765-2013, 2013.
651 Cheng, Y., Engling, G., Moosmaller, H., Arnott, W. P., Chen, L. W. A., Wold, C. E., Hao, W.
652 M., and He, K. B.: Light absorption by biomass burning source emissions, Atmos.
653 Environ., 127, 347-354, doi:10.1016/j.atmosenv.2015.12.045, 2016.
654 Chhabra, P. S., Ng, N. L., Canagaratna, M. R., Corrigan, A. L., Russell, L. M., Worsnop, D. R.,
655 Flagan, R. C., and Seinfeld, J. H.: Elemental composition and oxidation of chamber
656 organic aerosol, Atmos. Chem. Phys., 11, 8827-8845, doi:10.5194/acp-11-8827-2011,
657 2011.
658 Christian, T. J., Yokelson, R. J., Cardenas, B., Molina, L. T., Engling, G., and Hsu, S. C.: Trace
659 gas and particle emissions from domestic and industrial biofuel use and garbage burning
660 in central Mexico, Atmos. Chem. Phys., 10, 565-584, doi:10.5194/acp-10-565-2010, 2010.
661 Cubison, M. J., Ortega, A. M., Hayes, P. L., Farmer, D. K., Day, D., Lechner, M. J., Brune, W.
662 H., Apel, E., Diskin, G. S., Fisher, J. A., Fuelberg, H. E., Hecobian, A., Knapp, D. J.,
663 Mikoviny, T., Riemer, D., Sachse, G. W., Sessions, W., Weber, R. J., Weinheimer, A. J.,
664 Wisthaler, A., and Jimenez, J. L.: Effects of aging on organic aerosol from open biomass
665 burning smoke in aircraft and laboratory studies, Atmos. Chem. Phys., 11, 12049-12064,

doi:10.5194/acp-11-12049-2011, 2011.

DeCarlo, P. F., Slowik, J. G., Worsnop, D. R., Davidovits, P., and Jimenez, J. L.: Particle morphology and density characterization by combined mobility and aerodynamic diameter measurements. Part 1: Theory, Aerosol Sci. Technol., 38, 1185-1205, doi:10.1080/027868290903907, 2004.

DeCarlo, P. F., Kimmel, J. R., Trimborn, A., Northway, M. J., Jayne, J. T., Aiken, A. C., Gonin, M., Fuhrer, K., Horvath, T., Docherty, K. S., Worsnop, D. R., and Jimenez, J. L.: Field-deployable, high-resolution, time-of-flight aerosol mass spectrometer, Anal. Chem., 78, 8281-8289, doi:10.1021/ac061249n, 2006.

Deng, W., Liu, T., Zhang, Y., Situ, S., Hu, Q., He, Q., Zhang, Z., Lü, S., Bi, X., Wang, X., Boreave, A., George, C., Ding, X., and Wang, X.: Secondary organic aerosol formation from photo-oxidation of toluene with NO_x and SO_2: Chamber simulation with purified air versus urban ambient air as matrix, Atmos. Environ., 150, 67-76, doi:10.1016/j.atmosenv.2016.11.047, 2017.

Dhammapala, R., Claiborn, C., Jimenez, J., Corkill, J., Gullett, B., Simpson, C., and Paulsen, M.: Emission factors of PAHs, methoxyphenols, levoglucosan, elemental carbon and organic carbon from simulated wheat and Kentucky bluegrass stubble burns, Atmos. Environ., 41, 2660-2669, doi:10.1016/j.atmosenv.2006.11.023, 2007.

Ding, X., He, Q.-F., Shen, R.-Q., Yu, Q.-Q., Zhang, Y.-Q., Xin, J.-Y., Wen, T.-X., and Wang, X.-M.: Spatial and seasonal variations of isoprene secondary organic aerosol in China: Significant impact of biomass burning during winter, Sci. Rep., 6, 20411, doi:10.1038/srep20411, 2016a.

Ding, X., Zhang, Y.-Q., He, Q.-F., Yu, Q.-Q., Shen, R.-Q., Zhang, Y., Zhang, Z., Lyu, S.-J., Hu, Q.-H., Wang, Y.-S., Li, L.-F., Song, W., and Wang, X.-M.: Spatial and seasonal variations of secondary organic aerosol from terpenoids over China, J. Geophys. Res.-Atmos., 121,

14661–14678, doi:10.1002/2016JD025467, 2016b.

Ding, X., Zhang, Y.-Q., He, Q.-F., Yu, Q.-Q., Wang, J.-Q., Shen, R.-Q., Song, W., Wang, Y.-S., and Wang, X.-M.: Significant increase of aromatics-derived secondary organic aerosol during fall to winter in China, Environ. Sci. Technol., doi:10.1021/acs.est.6b06408, 2017.

Du, Q., Zhang, C., Mu, Y., Cheng, Y., Zhang, Y., Liu, C., Song, M., Tian, D., Liu, P., Liu, J., Xue, C., and Ye, C.: An important missing source of atmospheric carbonyl sulfide: Domestic coal combustion, Geophys. Res. Lett., 43, 8720-8727, doi:10.1002/2016gl070075, 2016.

Duncan, B. N., Bey, I., Chin, M., Mickley, L. J., Fairlie, T. D., Martin, R. V., and Matsueda, H.: Indonesian wildfires of 1997: Impact on tropospheric chemistry, J. Geophys. Res.-Atmos., 108, 25, doi:10.1029/2002jd003195, 2003.

Ervens, B., Turpin, B. J., and Weber, R. J.: Secondary organic aerosol formation in cloud droplets and aqueous particles (aqSOA): a review of laboratory, field and model studies, Atmos. Chem. Phys., 11, 11069-11102, doi:10.5194/acp-11-11069-2011, 2011.

Food and Agriculture Organization of the United Nation: Emissions of methane and nitrous oxide from the on-site combustion of crop residues, http://faostat3.fao.org/browse/G1/GB/E, last accessed: 6 April 2017.

Ge, S., Xu, Y., and Jia, L.: Secondary organic aerosol formation from ethyne in the presence of NaCl in a smog chamber, Environ. Chem., 13, 699-710, doi:10.1071/en15155, 2016.

Ge, S., Xu, Y., and Jia, L.: Secondary organic aerosol formation from propylene irradiations in a chamber study, Atmos. Environ., 157, 146-155, doi:10.1016/j.atmosenv.2017.03.019, 2017.

Giordano, M. R., Short, D. Z., Hosseini, S., Lichtenberg, W., and Asa-Awuku, A. A.: Changes in droplet surface tension affect the observed hygroscopicity of photochemically aged biomass burning aerosol, Environ. Sci. Technol., 47, 10980-10986,

716 doi:10.1021/es401867j, 2013.
717 Gómez Alvarez, E., Borras, E., Viidanoja, J., and Hjorth, J.: Unsaturated dicarbonyl products
718 from the OH-initiated photo-oxidation of furan, 2-methylfuran and 3-methylfuran, Atmos.
719 Environ., 43, 1603-1612, doi:10.1016/j.atmosenv.2008.12.019, 2009.
720 Grieshop, A. P., Donahue, N. M., and Robinson, A. L.: Laboratory investigation of
721 photochemical oxidation of organic aerosol from wood fires 2: analysis of aerosol mass
722 spectrometer data, Atmos. Chem. Phys., 9, 2227-2240, doi:10.5194/acp-9-2227-2009,
723 2009a.
724 Grieshop, A. P., Logue, J. M., Donahue, N. M., and Robinson, A. L.: Laboratory investigation
725 of photochemical oxidation of organic aerosol from wood fires 1: measurement and
726 simulation of organic aerosol evolution, Atmos. Chem. Phys., 9, 1263-1277,
727 doi:10.5194/acp-9-1263-2009, 2009b.
728 Hall, D., Wu, C. Y., Hsu, Y. M., Stormer, J., Engling, G., Capeto, K., Wang, J., Brown, S., Li,
729 H. W., and Yu, K. M.: PAHs, carbonyls, VOCs and $PM_{2.5}$ emission factors for pre-harvest
730 burning of Florida sugarcane, Atmos. Environ., 55, 164-172,
731 doi:10.1016/j.atmosenv.2012.03.034, 2012.
732 Hatch, L. E., Yokelson, R. J., Stockwell, C. E., Veres, P. R., Simpson, I. J., Blake, D. R., Orlando,
733 J. J., and Barsanti, K. C.: Multi-instrument comparison and compilation of non-methane
734 organic gas emissions from biomass burning and implications for smoke-derived
735 secondary organic aerosol precursors, Atmos. Chem. Phys., 17, 1471-1489,
736 doi:10.5194/acp-17-1471-2017, 2017.
737 Hayes, P. L., Ortega, A. M., Cubison, M. J., Froyd, K. D., Zhao, Y., Cliff, S. S., Hu, W. W.,
738 Toohey, D. W., Flynn, J. H., Lefer, B. L., Grossberg, N., Alvarez, S., Rappenglueck, B.,
739 Taylor, J. W., Allan, J. D., Holloway, J. S., Gilman, J. B., Kuster, W. C., De Gouw, J. A.,
740 Massoli, P., Zhang, X., Liu, J., Weber, R. J., Corrigan, A. L., Russell, L. M., Isaacman, G.,

741 Worton, D. R., Kreisberg, N. M., Goldstein, A. H., Thalman, R., Waxman, E. M.,
742 Volkamer, R., Lin, Y. H., Surratt, J. D., Kleindienst, T. E., Offenberg, J. H., Dusanter, S.,
743 Griffith, S., Stevens, P. S., Brioude, J., Angevine, W. M., and Jimenez, J. L.: Organic
744 aerosol composition and sources in Pasadena, California, during the 2010 CalNex
745 campaign, J. Geophys. Res.-Atmos., 118, 9233-9257, doi:10.1002/jgrd.50530, 2013.
746 Heald, C. L., Kroll, J. H., Jimenez, J. L., Docherty, K. S., DeCarlo, P. F., Aiken, A. C., Chen,
747 Q., Martin, S. T., Farmer, D. K., and Artaxo, P.: A simplified description of the evolution
748 of organic aerosol composition in the atmosphere, Geophys. Res. Lett., 37, L08803,
749 doi:10.1029/2010gl042737, 2010.
750 Hennigan, C. J., Miracolo, M. A., Engelhart, G. J., May, A. A., Presto, A. A., Lee, T., Sullivan,
751 A. P., McMeeking, G. R., Coe, H., Wold, C. E., Hao, W. M., Gilman, J. B., Kuster, W. C.,
752 de Gouw, J., Schichtel, B. A., Collett, J. L., Kreidenweis, S. M., and Robinson, A. L.:
753 Chemical and physical transformations of organic aerosol from the photo-oxidation of
754 open biomass burning emissions in an environmental chamber, Atmos. Chem. Phys., 11,
755 7669-7686, doi:10.5194/acp-11-7669-2011, 2011.
756 Henry, K. M., Lohaus, T., and Donahue, N. M.: Organic aerosol yields from α-pinene oxidation:
757 bridging the gap between first-generation yields and aging chemistry, Environ. Sci.
758 Technol., 46, 12347-12354, doi:10.1021/es302060y, 2012.
759 Heringa, M. F., DeCarlo, P. F., Chirico, R., Tritscher, T., Dommen, J., Weingartner, E., Richter,
760 R., Wehrle, G., Prévôt, A. S. H., and Baltensperger, U.: Investigations of primary and
761 secondary particulate matter of different wood combustion appliances with a high-
762 resolution time-of-flight aerosol mass spectrometer, Atmos. Chem. Phys., 11, 5945-5957,
763 doi:10.5194/acp-11-5945-2011, 2011.
764 Hildebrandt, L., Donahue, N. M., and Pandis, S. N.: High formation of secondary organic
765 aerosol from the photo-oxidation of toluene, Atmos. Chem. Phys., 9, 2973-2986,

766 doi:10.5194/acp-9-2973-2009, 2009.
767 Hossain, A., Park, S., Kim, J. S., and Park, K.: Volatility and mixing states of ultrafine particles
768 from biomass burning, J. Hazard. Mater., 205, 189-197,
769 doi:10.1016/j.jhazmat.2011.12.061, 2012.
770 Hosseini, S., Urbanski, S. P., Dixit, P., Qi, L., Burling, I. R., Yokelson, R. J., Johnson, T. J.,
771 Shrivastava, M., Jung, H. S., Weise, D. R., Miller, J. W., and Cocker, D. R.: Laboratory
772 characterization of PM emissions from combustion of wildland biomass fuels, J. Geophys.
773 Res.-Atmos., 118, 9914-9929, doi:10.1002/jgrd.50481, 2013.
774 Huang, R. J., Zhang, Y. L., Bozzetti, C., Ho, K. F., Cao, J. J., Han, Y. M., Daellenbach, K. R.,
775 Slowik, J. G., Platt, S. M., Canonaco, F., Zotter, P., Wolf, R., Pieber, S. M., Bruns, E. A.,
776 Crippa, M., Ciarelli, G., Piazzalunga, A., Schwikowski, M., Abbaszade, G., Schnelle-
777 Kreis, J., Zimmermann, R., An, Z. S., Szidat, S., Baltensperger, U., El Haddad, I., and
778 Prevot, A. S. H.: High secondary aerosol contribution to particulate pollution during haze
779 events in China, Nature, 514, 218-222, doi:10.1038/nature13774, 2014.
780 Huang, X., Ding, A., Liu, L., Liu, Q., Ding, K., Niu, X., Nie, W., Xu, Z., Chi, X., Wang, M.,
781 Sun, J., Guo, W., and Fu, C.: Effects of aerosol-radiation interaction on precipitation
782 during biomass-burning season in East China, Atmos. Chem. Phys., 16, 10063-10082,
783 doi:10.5194/acp-16-10063-2016, 2016.
784 Huang, Y., Shen, H. Z., Chen, Y. L., Zhong, Q. R., Chen, H., Wang, R., Shen, G. F., Liu, J. F.,
785 Li, B. G., and Tao, S.: Global organic carbon emissions from primary sources from 1960
786 to 2009, Atmos. Environ., 122, 505-512, doi:10.1016/j.atmosenv.2015.10.017, 2015.
787 Huang, Z., Zhang, Y., Yan, Q., Zhang, Z., and Wang, X.: Real-time monitoring of respiratory
788 absorption factors of volatile organic compounds in ambient air by proton transfer reaction
789 time-of-flight mass spectrometry, J. Hazard. Mater., 320, 547-555,
790 doi:10.1016/j.jhazmat.2016.08.064, 2016.

Huffman, J. A., Docherty, K. S., Mohr, C., Cubison, M. J., Ulbrich, I. M., Ziemann, P. J., Onasch, T. B., and Jimenez, J. L.: Chemically-resolved volatility measurements of organic aerosol from different sources, Environ. Sci. Technol., 43, 5351-5357, doi:10.1021/es803539d, 2009.

Jathar, S. H., Gordon, T. D., Hennigan, C. J., Pye, H. O. T., Pouliot, G., Adams, P. J., Donahue, N. M., and Robinson, A. L.: Unspeciated organic emissions from combustion sources and their influence on the secondary organic aerosol budget in the United States, Proc. Natl. Acad. Sci. U. S. A., 111, 10473-10478, doi:10.1073/pnas.1323740111, 2014.

Jia, L., and Xu, Y.: Ozone and secondary organic aerosol formation from Ethylene-NO_x-NaCl irradiations under different relative humidity conditions, J. Atmos. Chem., 73, 81-100, doi:10.1007/s10874-015-9317-1, 2016.

Jolleys, M. D., Coe, H., McFiggans, G., Capes, G., Allan, J. D., Crosier, J., Williams, P. I., Allen, G., Bower, K. N., Jimenez, J. L., Russell, L. M., Grutter, M., and Baumgardner, D.: Characterizing the aging of biomass burning organic aerosol by use of mixing ratios: a meta-analysis of four regions, Environ. Sci. Technol., 46, 13093-13102, doi:10.1021/es302386v, 2012.

Kim Oanh, N. T., Ly, B. T., Tipayarom, D., Manandhar, B. R., Prapat, P., Simpson, C. D., and Sally Liu, L. J.: Characterization of particulate matter emission from open burning of rice straw, Atmos. Environ., 45, 493-502, doi:10.1016/j.atmosenv.2010.09.023, 2011.

Kim Oanh, N. T., Tipayarom, A., Bich, T. L., Tipayarom, D., Simpson, C. D., Hardie, D., and Sally Liu, L. J.: Characterization of gaseous and semi-volatile organic compounds emitted from field burning of rice straw, Atmos. Environ., 119, 182-191, doi:10.1016/j.atmosenv.2015.08.005, 2015.

Kirchstetter, T. W., and Novakov, T.: Controlled generation of black carbon particles from a diffusion flame and applications in evaluating black carbon measurement methods, Atmos.

816 Environ., 41, 1874-1888, doi:10.1016/j.atmosenv.2006.10.067, 2007.
817 Koren, I., Kaufman, Y. J., Remer, L. A., and Martins, J. V.: Measurement of the effect of
818 Amazon smoke on inhibition of cloud formation, Science, 303, 1342-1345,
819 doi:10.1126/science.1089424, 2004.
820 Kroll, J. H., Donahue, N. M., Jimenez, J. L., Kessler, S. H., Canagaratna, M. R., Wilson, K. R.,
821 Altieri, K. E., Mazzoleni, L. R., Wozniak, A. S., and Bluhm, H.: Carbon oxidation state
822 as a metric for describing the chemistry of atmospheric organic aerosol, Nat. Chem., 3,
823 133-139, doi:10.1038/nchem.948, 2011.
824 Lambe, A. T., Ahern, A. T., Williams, L. R., Slowik, J. G., Wong, J. P. S., Abbatt, J. P. D.,
825 Brune, W. H., Ng, N. L., Wright, J. P., Croasdale, D. R., Worsnop, D. R., Davidovits, P.,
826 and Onasch, T. B.: Characterization of aerosol photooxidation flow reactors:
827 heterogeneous oxidation, secondary organic aerosol formation and cloud condensation
828 nuclei activity measurements, Atmos. Meas. Tech., 4, 445-461, doi:10.5194/amt-4-445-
829 2011, 2011.
830 Laskin, A., Laskin, J., and Nizkorodov, S. A.: Chemistry of atmospheric brown carbon, Chem.
831 Rev., 115, 4335-4382, doi:10.1021/cr5006167, 2015.
832 Li, C., Ma, Z., Chen, J., Wang, X., Ye, X., Wang, L., Yang, X., Kan, H., Donaldson, D. J., and
833 Mellouki, A.: Evolution of biomass burning smoke particles in the dark, Atmos. Environ.,
834 120, 244-252, doi:10.1016/j.atmosenv.2015.09.003, 2015.
835 Li, C., Hu, Y., Zhang, F., Chen, J., Ma, Z., Ye, X., Yang, X., Wang, L., Tang, X., Zhang, R., Mu,
836 M., Wang, G., Kan, H., Wang, X., and Mellouki, A.: Multi-pollutant emissions from the
837 burning of major agricultural residues in China and the related health-economic effects,
838 Atmos. Chem. Phys., 17, 4957-4988, doi:10.5194/acp-17-4957-2017, 2017.
839 Li, J., Bo, Y., and Xie, S. D.: Estimating emissions from crop residue open burning in China
840 based on statistics and MODIS fire products, J. Environ. Sci., 44, 158-170,

doi:10.1016/j.jes.2015.08.024, 2016.

Li, Q., Li, X. H., Jiang, J. K., Duan, L., Ge, S., Zhang, Q., Deng, J. G., Wang, S. X., and Hao, J. M.: Semi-coke briquettes: towards reducing emissions of primary $PM_{2.5}$, particulate carbon, and carbon monoxide from household coal combustion in China, Sci. Rep., 6, 10, doi:10.1038/srep19306, 2016.

Li, X. G., Wang, S. X., Duan, L., Hao, J., Li, C., Chen, Y. S., and Yang, L.: Particulate and trace gas emissions from open burning of wheat straw and corn stover in China, Environ. Sci. Technol., 41, 6052-6058, doi:10.1021/es0705137, 2007.

Li, X. H., Wang, S. X., Duan, L., and Hao, J. M.: Characterization of non-methane hydrocarbons emitted from open burning of wheat straw and corn stover in China, Environ. Res. Lett., 4, 7, doi:10.1088/1748-9326/4/4/044015, 2009.

Lim, Y. B., Tan, Y., and Turpin, B. J.: Chemical insights, explicit chemistry, and yields of secondary organic aerosol from OH radical oxidation of methylglyoxal and glyoxal in the aqueous phase, Atmos. Chem. Phys., 13, 8651-8667, doi:10.5194/acp-13-8651-2013, 2013.

Lipsky, E. M., and Robinson, A. L.: Effects of dilution on fine particle mass and partitioning of semivolatile organics in diesel exhaust and wood smoke, Environ. Sci. Technol., 40, 155-162, doi:10.1021/es050319p, 2006.

Liu, C., Zhang, C., Mu, Y., Liu, J., and Zhang, Y.: Emission of volatile organic compounds from domestic coal stove with the actual alternation of flaming and smoldering combustion processes, Environ. Pollut., 221, 385-391, doi:10.1016/j.envpol.2016.11.089, 2017.

Liu, J., Mauzerall, D. L., Chen, Q., Zhang, Q., Song, Y., Peng, W., Klimont, Z., Qiu, X., Zhang, S., Hu, M., Lin, W., Smith, K. R., and Zhu, T.: Air pollutant emissions from Chinese households: A major and underappreciated ambient pollution source, Proc. Natl. Acad.

Sci., doi:10.1073/pnas.1604537113, 2016.

Liu, T., Wang, X., Deng, W., Hu, Q., Ding, X., Zhang, Y., He, Q., Zhang, Z., Lu, S., Bi, X., Chen, J., and Yu, J.: Secondary organic aerosol formation from photochemical aging of light-duty gasoline vehicle exhausts in a smog chamber, Atmos. Chem. Phys., 15, 9049-9062, doi:10.5194/acp-15-9049-2015, 2015.

Liu, X. X., Zhang, Y., Huey, L. G., Yokelson, R. J., Wang, Y., Jimenez, J. L., Campuzano-Jost, P., Beyersdorf, A. J., Blake, D. R., Choi, Y., St Clair, J. M., Crounse, J. D., Day, D. A., Diskin, G. S., Fried, A., Hall, S. R., Hanisco, T. F., King, L. E., Meinardi, S., Mikoviny, T., Palm, B. B., Peischl, J., Perring, A. E., Pollack, I. B., Ryerson, T. B., Sachse, G., Schwarz, J. P., Simpson, I. J., Tanner, D. J., Thornhill, K. L., Ullmann, K., Weber, R. J., Wennberg, P. O., Wisthaler, A., Wolfe, G. M., and Ziemba, L. D.: Agricultural fires in the southeastern US during SEAC^{4}RS: Emissions of trace gases and particles and evolution of ozone, reactive nitrogen, and organic aerosol, J. Geophys. Res.-Atmos., 121, 7383-7414, doi:10.1002/2016jd025040, 2016.

Martin, M., Tritscher, T., Juranyi, Z., Heringa, M. F., Sierau, B., Weingartner, E., Chirico, R., Gysel, M., Prevot, A. S. H., Baltensperger, U., and Lohmann, U.: Hygroscopic properties of fresh and aged wood burning particles, J. Aerosol Sci., 56, 15-29, doi:10.1016/j.jaerosci.2012.08.006, 2013.

May, A. A., Levin, E. J. T., Hennigan, C. J., Riipinen, I., Lee, T., Collett, J. L., Jr., Jimenez, J. L., Kreidenweis, S. M., and Robinson, A. L.: Gas-particle partitioning of primary organic aerosol emissions: 3. Biomass burning, J. Geophys. Res.-Atmos., 118, 11327-11338, doi:10.1002/jgrd.50828, 2013.

May, A. A., Lee, T., McMeeking, G. R., Akagi, S., Sullivan, A. P., Urbanski, S., Yokelson, R. J., and Kreidenweis, S. M.: Observations and analysis of organic aerosol evolution in some prescribed fire smoke plumes, Atmos. Chem. Phys., 15, 6323-6335, doi:10.5194/acp-15-

6323-2015, 2015.

McMurry, P. H., and Grosjean, D.: Gas and aerosol wall losses in Teflon film smog chambers, Environ. Sci. Technol., 19, 1176-1182, doi:10.1021/es00142a006, 1985.

Müller, M., Anderson, B. E., Beyersdorf, A. J., Crawford, J. H., Diskin, G. S., Eichler, P., Fried, A., Keutsch, F. N., Mikoviny, T., Thornhill, K. L., Walega, J. G., Weinheimer, A. J., Yang, M., Yokelson, R. J., and Wisthaler, A.: In situ measurements and modeling of reactive trace gases in a small biomass burning plume, Atmos. Chem. Phys., 16, 3813-3824, doi:10.5194/acp-16-3813-2016, 2016.

Nakao, S., Clark, C., Tang, P., Sato, K., and Iii, D. C.: Secondary organic aerosol formation from phenolic compounds in the absence of NO_x, Atmos. Chem. Phys., 11, 2025-2055, doi:10.5194/acp-11-10649-2011, 2011.

National bureau of statistics of people's republic of China.: China Energy Statistical Yearbook 2013, China Stat. Press, Beijing, 2014.

National bureau of statistics of people's republic of China.: The statistical communiqu on national economy and social development in 2015, http://www.stats.gov.cn/tjsj/zxfb/201602/t20160229_1323991.html, last accessed: 27 ~~April~~ September 2017.

Ng, N. L., Chhabra, P. S., Chan, A. W. H., Surratt, J. D., Kroll, J. H., Kwan, A. J., McCabe, D. C., Wennberg, P. O., Sorooshian, A., Murphy, S. M., Dalleska, N. F., Flagan, R. C., and Seinfeld, J. H.: Effect of NO_x level on secondary organic aerosol (SOA) formation from the photooxidation of terpenes, Atmos. Chem. Phys., 7, 5159-5174, doi:10.5194/acp-7-5159-2007, 2007a.

Ng, N. L., Kroll, J. H., Chan, A. W. H., Chhabra, P. S., Flagan, R. C., and Seinfeld, J. H.: Secondary organic aerosol formation from m-xylene, toluene, and benzene, Atmos. Chem. Phys., 7, 3909-3922, doi:10.5194/acp-7-3909-2007, 2007b.

916 Ng, N. L., Canagaratna, M. R., Zhang, Q., Jimenez, J. L., Tian, J., Ulbrich, I. M., Kroll, J. H.,
917 Docherty, K. S., Chhabra, P. S., Bahreini, R., Murphy, S. M., Seinfeld, J. H., Hildebrandt,
918 L., Donahue, N. M., DeCarlo, P. F., Lanz, V. A., Prevot, A. S. H., Dinar, E., Rudich, Y.,
919 and Worsnop, D. R.: Organic aerosol components observed in Northern Hemispheric
920 datasets from Aerosol Mass Spectrometry, Atmos. Chem. Phys., 10, 4625-4641,
921 doi:10.5194/acp-10-4625-2010, 2010.
922 Ng, N. L., Canagaratna, M. R., Jimenez, J. L., Chhabra, P. S., Seinfeld, J. H., and Worsnop, D.
923 R.: Changes in organic aerosol composition with aging inferred from aerosol mass spectra,
924 Atmos. Chem. Phys., 11, 6465-6474, doi:10.5194/acp-11-6465-2011, 2011a.
925 Ng, N. L., Canagaratna, M. R., Jimenez, J. L., Zhang, Q., Ulbrich, I. M., and Worsnop, D. R.:
926 Real-Time Methods for estimating organic cComponent mass concentrations from aerosol
927 mass spectrometer data, Environ. Sci. Technol., 45, 910-916, doi:10.1021/es102951k,
928 2011b.
929 Ni, H. Y., Han, Y. M., Cao, J. J., Chen, L. W. A., Tian, J., Wang, X. L., Chow, J. C., Watson, J.
930 G., Wang, Q. Y., Wang, P., Li, H., and Huang, R. J.: Emission characteristics of
931 carbonaceous particles and trace gases from open burning of crop residues in China,
932 Atmos. Environ., 123, 399-406, doi:10.1016/j.atmosenv.2015.05.007, 2015.
933 Niu, H. Y., Cheng, W. J., Hu, W., and Pian, W.: Characteristics of individual particles in a severe
934 short-period haze episode induced by biomass burning in Beijing, Atmos. Pollut. Res., 7,
935 1072-1081, doi:10.1016/j.apr.2016.05.011, 2016.
936 Ortega, A. M., Day, D. A., Cubison, M. J., Brune, W. H., Bon, D., de Gouw, J. A., and Jimenez,
937 J. L.: Secondary organic aerosol formation and primary organic aerosol oxidation from
938 biomass-burning smoke in a flow reactor during FLAME-3, Atmos. Chem. Phys., 13,
939 11551-11571, doi:10.5194/acp-13-11551-2013, 2013.
940 Pan, X., Kanaya, Y., Tanimoto, H., Inomata, S., Wang, Z., Kudo, S., and Uno, I.: Examining

the major contributors of ozone pollution in a rural area of the Yangtze River Delta region during harvest season, Atmos. Chem. Phys., 15, 6101-6111, doi:10.5194/acp-15-6101-2015, 2015.

Presto, A. A., Miracolo, M. A., Kroll, J. H., Worsnop, D. R., Robinson, A. L., and Donahue, N. M.: Intermediate-volatility organic compounds: A potential source of ambient oxidized organic aerosol, Environ. Sci. Technol., 43, 4744-4749, doi:10.1021/es803219q, 2009.

Real, E., Law, K. S., Weinzierl, B., Fiebig, M., Petzold, A., Wild, O., Methven, J., Arnold, S., Stohl, A., Huntrieser, H., Roiger, A., Schlager, H., Stewart, D., Avery, M., Sachse, G., Browell, E., Ferrare, R., and Blake, D.: Processes influencing ozone levels in Alaskan forest fire plumes during long-range transport over the North Atlantic, J. Geophys. Res.-Atmos., 112, doi:10.1029/2006jd007576, 2007.

Robinson, A. L., Donahue, N. M., Shrivastava, M. K., Weitkamp, E. A., Sage, A. M., Grieshop, A. P., Lane, T. E., Pierce, J. R., and Pandis, S. N.: Rethinking organic aerosols: semivolatile emissions and photochemical aging, Science, 315, 1259-1262, doi:10.1126/science.1133061, 2007.

Sanchis, E., Ferrer, M., Calvet, S., Coscolla, C., Yusa, V., and Cambra-Lopez, M.: Gaseous and particulate emission profiles during controlled rice straw burning, Atmos. Environ., 98, 25-31, doi:10.1016/j.atmosenv.2014.07.062, 2014.

Schmid, O., Artaxo, P., Arnott, W. P., Chand, D., Gatti, L. V., Frank, G. P., Hoffer, A., Schnaiter, M., and Andreae, M. O.: Spectral light absorption by ambient aerosols influenced by biomass burning in the Amazon Basin. I: Comparison and field calibration of absorption measurement techniques, Atmos. Chem. Phys., 6, 3443-3462, doi:10.5194/acp-6-3443-2006, 2006.

Schmid, O., Karg, E., Hagen, D. E., Whitefield, P. D., and Ferron, G. A.: On the effective density of non-spherical particles as derived from combined measurements of

966 aerodynamic and mobility equivalent size, J. Aerosol Sci., 38, 431-443,
967 doi:10.1016/j.jaerosci.2007.01.002, 2007.
968 Shahid, I., Kistler, M., Mukhtar, A., Cruz, C. R. S., Bauer, H., and Puxbaum, H.: Chemical
969 composition of particles from traditional burning of Pakistani wood species, Atmos.
970 Environ., 121, 35-41, doi:10.1016/j.atmosenv.2015.01.041, 2015.
971 Shakya, K. M., and Griffin, R. J.: Secondary organic aerosol from photooxidation of polycyclic
972 aromatic hydrocarbons, Environ. Sci. Technol., 44, 8134-8139, doi:10.1021/es1019417,
973 2010.
974 Shrivastava, M., Easter, R. C., Liu, X. H., Zelenyuk, A., Singh, B., Zhang, K., Ma, P. L., Chand,
975 D., Ghan, S., Jimenez, J. L., Zhang, Q., Fast, J., Rasch, P. J., and Tiitta, P.: Global
976 transformation and fate of SOA: Implications of low-volatility SOA and gas-phase
977 fragmentation reactions, J. Geophys. Res.-Atmos., 120, 4169-4195,
978 doi:10.1002/2014jd022563, 2015.
979 Spracklen, D. V., Jimenez, J. L., Carslaw, K. S., Worsnop, D. R., Evans, M. J., Mann, G. W.,
980 Zhang, Q., Canagaratna, M. R., Allan, J., Coe, H., McFiggans, G., Rap, A., and Forster,
981 P.: Aerosol mass spectrometer constraint on the global secondary organic aerosol budget,
982 Atmos. Chem. Phys., 11, 12109-12136, doi:10.5194/acp-11-12109-2011, 2011.
983 Stockwell, C. E., Yokelson, R. J., Kreidenweis, S. M., Robinson, A. L., DeMott, P. J., Sullivan,
984 R. C., Reardon, J., Ryan, K. C., Griffith, D. W. T., and Stevens, L.: Trace gas emissions
985 from combustion of peat, crop residue, domestic biofuels, grasses, and other fuels:
986 configuration and Fourier transform infrared (FTIR) component of the fourth Fire Lab at
987 Missoula Experiment (FLAME-4), Atmos. Chem. Phys., 14, 9727-9754,
988 doi:10.5194/acp-14-9727-2014, 2014.
989 Stockwell, C. E., Veres, P. R., Williams, J., and Yokelson, R. J.: Characterization of biomass
990 burning emissions from cooking fires, peat, crop residue, and other fuels with high-

resolution proton-transfer-reaction time-of-flight mass spectrometry, Atmos. Chem. Phys., 15, 845-865, doi:10.5194/acp-15-845-2015, 2015.

Stockwell, C. E., Christian, T. J., Goetz, J. D., Jayarathne, T., Bhave, P. V., Praveen, P. S., Adhikari, S., Maharjan, R., DeCarlo, P. F., Stone, E. A., Saikawa, E., Blake, D. R., Simpson, I. J., Yokelson, R. J., and Panday, A. K.: Nepal Ambient Monitoring and Source Testing Experiment (NAMaSTE): emissions of trace gases and light-absorbing carbon from wood and dung cooking fires, garbage and crop residue burning, brick kilns, and other sources, Atmos. Chem. Phys., 16, 11043-11081, 10.5194/acp-16-11043-2016, 2016.

Streets, D. G., Yarber, K. F., Woo, J. H., and Carmichael, G. R.: Biomass burning in Asia: Annual and seasonal estimates and atmospheric emissions, Global Biogeochem. Cy., 17, 20, doi:10.1029/2003gb002040, 2003.

Takekawa, H., Minoura, H., and Yamazaki, S.: Temperature dependence of secondary organic aerosol formation by photo-oxidation of hydrocarbons, Atmos. Environ., 37, 3413-3424, doi:10.1016/s1352-2310(03)00359-5, 2003.

Tariq, S., ul-Haq, Z., and Ali, M.: Satellite and ground-based remote sensing of aerosols during intense haze event of October 2013 over lahore, Pakistan, Asia-Pac. J. Atmos. Sci., 52, 25-33, doi:10.1007/s13143-015-0084-3, 2016.

Tkacik, D. S., Robinson, E. S., Ahern, A., Saleh, R., Stockwell, C., Veres, P., Simpson, I. J., Meinardi, S., Blake, D. R., Yokelson, R. J., Presto, A. A., Sullivan, R. C., Donahue, N. M., and Robinson, A. L.: A dual-chamber method for quantifying the effects of atmospheric perturbations on secondary organic aerosol formation from biomass burning emissions, J. Geophys. Res.-Atmos., 122, 6043-6058, doi:10.1002/2016JD025784, 2017.

Thompson, A. M., Witte, J. C., Hudson, R. D., Guo, H., Herman, J. R., and Fujiwara, M.: Tropical tropospheric ozone and biomass burning, Science, 291, 2128-2132, doi:10.1126/science.291.5511.2128, 2001.

1016 Tian, H., Zhao, D., and Wang, Y.: Emission inventories of atmospheric pollutants discharged
1017 from biomass burning in China, Acta Sci. Circumst., 31, 349-357 in Chinese, 2011.
1018 Tissari, J., Lyyranen, J., Hytonen, K., Sippula, O., Tapper, U., Frey, A., Saarnio, K., Pennanen,
1019 A. S., Hillamo, R., Salonen, R. O., Hirvonen, M. R., and Jokiniemi, J.: Fine particle and
1020 gaseous emissions from normal and smouldering wood combustion in a conventional
1021 masonry heater, Atmos. Environ., 42, 7862-7873, doi:10.1016/j.atmosenv.2008.07.019,
1022 2008.
1023 Tiitta, P., Leskinen, A., Hao, L., Yli-Pirila, P., Kortelainen, M., Grigonyte, J., Tissari, J.,
1024 Lamberg, H., Hartikainen, A., Kuuspalo, K., Kortelainen, A.-M., Virtanen, A., Lehtinen,
1025 K. E. J., Komppula, M., Pieber, S., Prevot, A. S. H., Onasch, T. B., Worsnop, D. R., Czech,
1026 H., Zimmermann, R., Jokiniemi, J., and Sippula, O.: Transformation of logwood
1027 combustion emissions in a smog chamber: formation of secondary organic aerosol and
1028 changes in the primary organic aerosol upon daytime and nighttime aging, Atmos. Chem.
1029 Phys., 16, 13251-13269, doi:10.5194/acp-16-13251-2016, 2016.
1030 Tsigaridis, K., Daskalakis, N., Kanakidou, M., Adams, P. J., Artaxo, P., Bahadur, R., Balkanski,
1031 Y., Bauer, S. E., Bellouin, N., Benedetti, A., Bergman, T., Berntsen, T. K., Beukes, J. P.,
1032 Bian, H., Carslaw, K. S., Chin, M., Curci, G., Diehl, T., Easter, R. C., Ghan, S. J., Gong,
1033 S. L., Hodzic, A., Hoyle, C. R., Iversen, T., Jathar, S., Jimenez, J. L., Kaiser, J. W.,
1034 Kirkevåg, A., Koch, D., Kokkola, H., Lee, Y. H., Lin, G., Liu, X., Luo, G., Ma, X., Mann,
1035 G. W., Mihalopoulos, N., Morcrette, J. J., Müller, J. F., Myhre, G., Myriokefalitakis, S.,
1036 Ng, N. L., O'Donnell, D., Penner, J. E., Pozzoli, L., Pringle, K. J., Russell, L. M., Schulz,
1037 M., Sciare, J., Seland, Ø., Shindell, D. T., Sillman, S., Skeie, R. B., Spracklen, D.,
1038 Stavrakou, T., Steenrod, S. D., Takemura, T., Tiitta, P., Tilmes, S., Tost, H., van Noije, T.,
1039 van Zyl, P. G., von Salzen, K., Yu, F., Wang, Z., Wang, Z., Zaveri, R. A., Zhang, H., Zhang,
1040 K., Zhang, Q., and Zhang, X.: The AeroCom evaluation and intercomparison of organic

aerosol in global models, Atmos. Chem. Phys., 14, 10845-10895, doi:10.5194/acp-14-10845-2014, 2014.

Wang, H., Lou, S., Huang, C., Qiao, L., Tang, X., Chen, C., Zeng, L., Wang, Q., Zhou, M., Lu, S., and Yu, X.: Source profiles of volatile organic compounds from biomass burning in Yangtze River Delta, China, Aerosol Air Qual. Res., 14, 818-828, doi:10.4209/aaqr.2013.05.0174, 2014.

Wang, X., and Wu, T.: Release of isoprene and monoterpenes during the aerobic decomposition of orange wastes from laboratory incubation experiments, Environ. Sci. Technol., 42, 3265-3270, doi:10.1021/es702999j, 2008.

Wang, X., Liu, T., Bernard, F., Ding, X., Wen, S., Zhang, Y., Zhang, Z., He, Q., Lu, S., Chen, J., Saunders, S., and Yu, J.: Design and characterization of a smog chamber for studying gas-phase chemical mechanisms and aerosol formation, Atmos. Meas. Tech., 7, 301-313, doi:10.5194/amt-7-301-2014, 2014.

Ward, D. E., Susott, R. A., Kauffman, J. B., Babbitt, R. E., Cummings, D. L., Dias, B., Holben, B. N., Kaufman, Y. J., Rasmussen, R. A., and Setzer, A. W.: Smoke and fire characteristics for cerrado and deforestation burns in Brazil: BASE-B Experiment, J. Geophys. Res.-Atmos., 97, 14601-14619, doi:10.1029/92JD01218, 1992.

Weimer, S., Alfarra, M. R., Schreiber, D., Mohr, M., Prevot, A. S. H., and Baltensperger, U.: Organic aerosol mass spectral signatures from wood-burning emissions: Influence of burning conditions and wood type, J. Geophys. Res.-Atmos., 113, doi:10.1029/2007jd009309, 2008.

Weitkamp, E. A., Sage, A. M., Pierce, J. R., Donahue, N. M., and Robinson, A. L.: Organic aerosol formation from photochemical oxidation of diesel exhaust in a smog chamber, Environ. Sci. Technol., 41, 6969-6975, doi:10.1021/es070193r, 2007.

Yee, L. D., Kautzman, K. E., Loza, C. L., Schilling, K. A., Coggon, M. M., Chhabra, P. S.,

1066 Chan, M. N., Chan, A. W. H., Hersey, S. P., Crounse, J. D., Wennberg, P. O., Flagan, R.
1067 C., and Seinfeld, J. H.: Secondary organic aerosol formation from biomass burning
1068 intermediates: phenol and methoxyphenols, Atmos. Chem. Phys., 13, 8019-8043,
1069 doi:10.5194/acp-13-8019-2013, 2013.
1070 Yi, Z. G., Wang, X. M., Sheng, G. Y., Zhang, D. Q., Zhou, G. Y., and Fu, J. M.: Soil uptake of
1071 carbonyl sulfide in subtropical forests with different successional stages in south China, J.
1072 Geophys. Res.-Atmos., 112, 11, doi:10.1029/2006jd008048, 2007.
1073 Yokelson, R. J., Christian, T. J., Karl, T. G., and Guenther, A.: The tropical forest and fire
1074 emissions experiment: laboratory fire measurements and synthesis of campaign data,
1075 Atmos. Chem. Phys., 8, 3509-3527, doi:10.5194/acp-8-3509-2008, 2008.
1076 Yokelson, R. J., Burling, I. R., Urbanski, S. P., Atlas, E. L., Adachi, K., Buseck, P. R.,
1077 Wiedinmyer, C., Akagi, S. K., Toohey, D. W., and Wold, C. E.: Trace gas and particle
1078 emissions from open biomass burning in Mexico, Atmos. Chem. Phys., 11, 6787-6808,
1079 doi:10.5194/acp-11-6787-2011, 2011.
1080 Zhang, H., Ye, X., Cheng, T., Chen, J., Yang, X., Wang, L., and Zhang, R.: A laboratory study
1081 of agricultural crop residue combustion in China: Emission factors and emission inventory,
1082 Atmos. Environ., 42, 8432-8441, doi:10.1016/j.atmosenv.2008.08.015, 2008.
1083 Zhang, H., Hu, D., Chen, J., Ye, X., Wang, S. X., Hao, J. M., Wang, L., Zhang, R., and An, Z.:
1084 Particle size distribution and polycyclic aromatic hydrocarbons emissions from
1085 agricultural crop residue burning, Environ. Sci. Technol., 45, 5477-5482,
1086 doi:10.1021/es1037904, 2011.
1087 Zhang, Q., Jimenez, J.L., Canagaratna, M.R., Ulbrich, I.M., Ng, N.L., Worsnop, D.R., Sun,
1088 Y.L.: Understanding atmospheric organic aerosols via factor analysis of aerosol mass
1089 spectrometry: a review, Anal. Bioanal. Chem., 401, 3045-3067, doi: 10.1007/s00216-011-
1090 5355-y, 2011

Zhang, Y. L., Guo, H., Wang, X. M., Simpson, I. J., Barletta, B., Blake, D. R., Meinardi, S., Rowland, F. S., Cheng, H. R., Saunders, S. M., and Lam, S. H. M.: Emission patterns and spatiotemporal variations of halocarbons in the Pearl River Delta region, southern China, J. Geophys. Res.-Atmos., 115, 16, doi:10.1029/2009jd013726, 2010.

Zhang, Y. L., Wang, X. M., Blake, D. R., Li, L. F., Zhang, Z., Wang, S. Y., Guo, H., Lee, F. S. C., Gao, B., Chan, L. Y., Wu, D., and Rowland, F. S.: Aromatic hydrocarbons as ozone precursors before and after outbreak of the 2008 financial crisis in the Pearl River Delta region, south China, J. Geophys. Res.-Atmos., 117, 16, doi:10.1029/2011jd017356, 2012.

Zhao, Y. L., Hennigan, C. J., May, A. A., Tkacik, D. S., de Gouw, J. A., Gilman, J. B., Kuster, W. C., Borbon, A., and Robinson, A. L.: Intermediate-volatility organic compounds: A large source of secondary organic aerosol, Environ. Sci. Technol., 48, 13743-13750, doi:10.1021/es5035188, 2014.

Zhu, Y. H., Yang, L. X., Chen, J. M., Wang, X. F., Xue, L. K., Sui, X., Wen, L., Xu, C. H., Yao, L., Zhang, J. M., Shao, M., Lu, S. H., and Wang, W. X.: Characteristics of ambient volatile organic compounds and the influence of biomass burning at a rural site in Northern China during summer 2013, Atmos. Environ., 124, 156-165, doi:10.1016/j.atmosenv.2015.08.097, 2016.

Table 1. Primary emission factors measured for agricultural residues burning. All the units are g kg^{-1}, except the unit for particle number (PN) is 10^{15} particle kg^{-1}. MCE: modified combustion efficiency; NMHCs: non-methane hydrocarbons; POA: primary organic aerosol; POC primary organic carbon; BC: black carbon.

	Rice		Corn		Wheat	
Species	This study (n=9)	Others	This study (n=6)	Others	This study (n=5)	Others
MCE	0.926±0.049		0.953±0.019		0.949±0.035	
CO_2	1262±81		1477±28		1423±60	
CO	63.5±41.4		46.1±19.2		48.6±33.0	
NO_x	1.47±0.61	3.51±0.38[a]	5.00±3.94	4.3±1.8[b]	3.08±0.93	3.3±1.7[b]; 2.27±0.04[a]
NH_3	0.45±0.15	0.95±0.65[a]; 4.10±1.24[c]	0.63±0.30	0.68±0.52[b]	0.22±0.19	0.37±0.14[b]; 0.21±0.14[a]
SO_2	0.07±0.07	0.18±0.31[d]; 0.37±0.27[e]; 1.27±0.35[a]	0.99±1.53	0.04±0.04[d]	0.72±0.34	0.04±0.04[d]; 0.73±0.15[a]
NMHCs	5.04±2.04	1.25[f]	2.47±2.11	1.59±0.43[g]	3.08±2.43	1.69±0.58[g]; 0.90[f]
PM	3.73±3.28	8.5±6.7[h]; 8.3±2.2[e]; 13.2±1.44[i]; 4.2[c]	5.44±3.43	12.2±5.4[h]; 11.7±1.0[b]; 5.36±0.55[i]	6.36±2.98	11.4±4.9[h]; 7.6±4.1[b]; 5.30±0.30[i]
PN	2.94±0.91	0.018±0.001[j]	7.29±4.17	0.017±0.001[j]	5.87±2.89	0.010±0.001[j]
POA	2.99±1.00		3.99±2.68		5.96±0.19	
POC	2.05±0.72	3.3±2.8[h]; 6.02±0.60[i]	2.52±1.66	6.3±3.6[h]; 3.9±1.7[b]; 2.06±0.34[i]	4.11±0.29	5.1±3.0[h]; 2.7±1.0[b]; 2.42±0.13[i]
BC	0.22±0.11	0.21±0.13[h]	0.24±0.09	0.28±0.09[h]; 0.35±0.10[b]	0.27±0.07	0.24±0.12[h]; 0.49±0.12[b]

[a] Stockwell et al., 2015; [b] Li et al., 2007, PM correspond to $PM_{2.5}$; [c] Christian et al., 2003; [d] Cao et al., 2008; [e] Kim Oanh et al., 2015, PM correspond to $PM_{2.5}$; [f] Wang et al., 2014, 56 NMHCs species summarized; [g] Li et al., 2009, 52 NMHCs species summarized; [h] Ni et al., 2015, PM correspond to $PM_{2.5}$; [i] Li et al., 2017, PM correspond to PM_1; [j] Zhang et al., 2008.

Table 2. Overview of important experimental conditions and key results in the photochemical oxidation experiments. The unit for OH exposure is 10^{10} molecule cm^{-3} s. NA: data was not available because no data was recorded in the W-mode.

NO.	Straw type	Temp (°C)	RH (%)	OH exposure	POA			Aged OA			OA ER
					O/C	H/C	OS_c	O/C	H/C	OS_c	
Burn 1	Rice	25.0±0.4	48.9±1.4	3.80	NA	NA	NA	NA	NA	NA	2.7
Burn 2	Rice	25.1±0.4	55.0±2.3	4.97	0.25	1.74	-1.25	0.50	1.65	-0.65	7.6
Burn 3	Corn	25.5±0.4	53.0±2.9	4.16	0.38	1.66	-0.89	0.60	1.66	-0.46	3.6
Burn 4	Corn	26.1±0.4	48.4±2.2	4.16	0.30	1.58	-0.97	0.65	1.57	-0.26	4.6
Burn 5	Wheat	25.3±0.5	52.8±2.2	3.20	0.20	1.66	-1.25	0.50	1.56	-0.55	2.4
Burn 6	Wheat	25.2±0.4	55.1±2.7	1.87	0.26	1.71	-1.20	0.53	1.66	-0.61	6.6

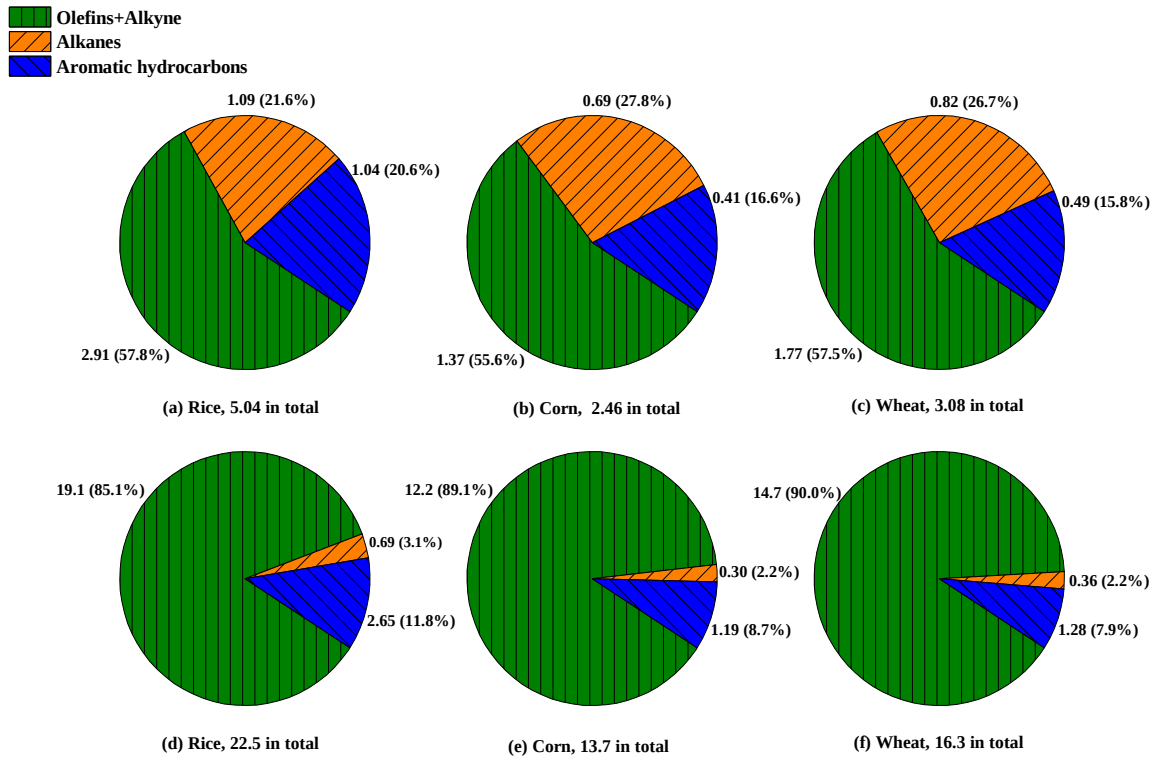

Figure 1. (a-c) Non-methane hydrocarbon (NMHC) compositions and (d-f) their relative contribution to ozone formation potential (OFP) for open burning of rice, corn and wheat straw.

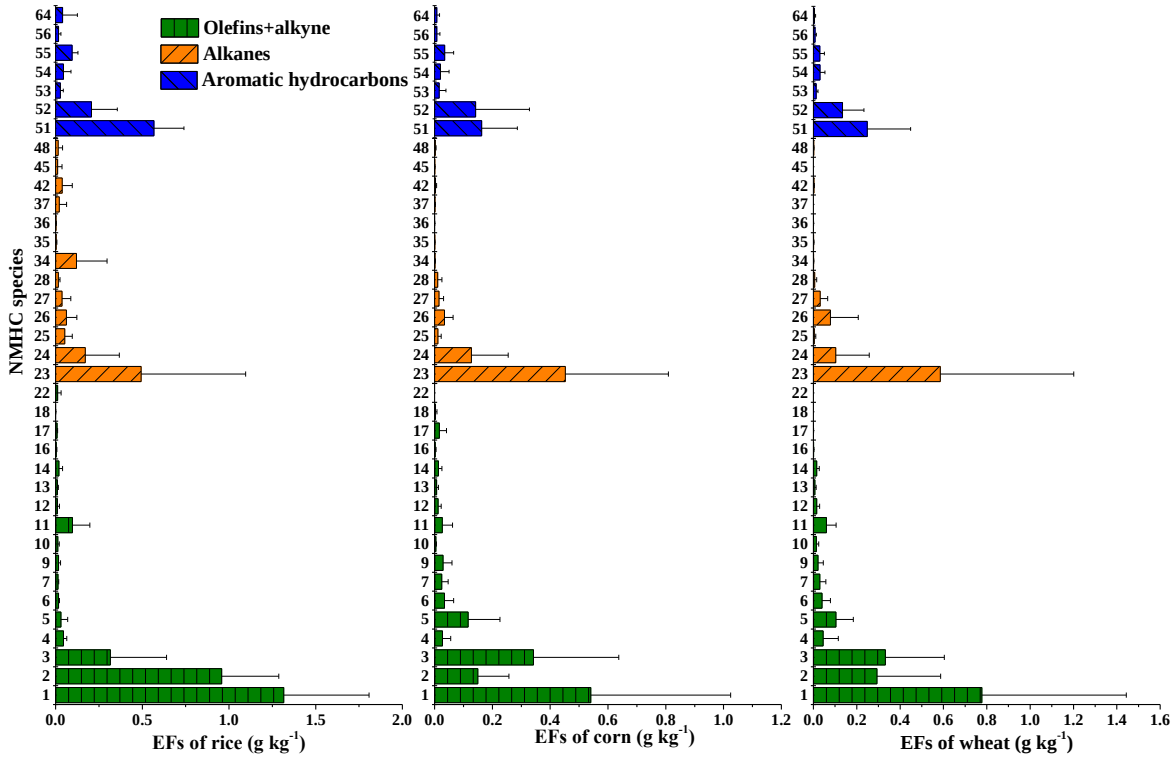

Figure 2. Emission factors (EFs) of NMHCs for straw burning of rice, corn and wheat. Only species with emission factors >0.01 g kg^{-1} are shown. The order of NMHC species is the same as Table S1 in which a comprehensive dataset of emission factors measured in this work is included.

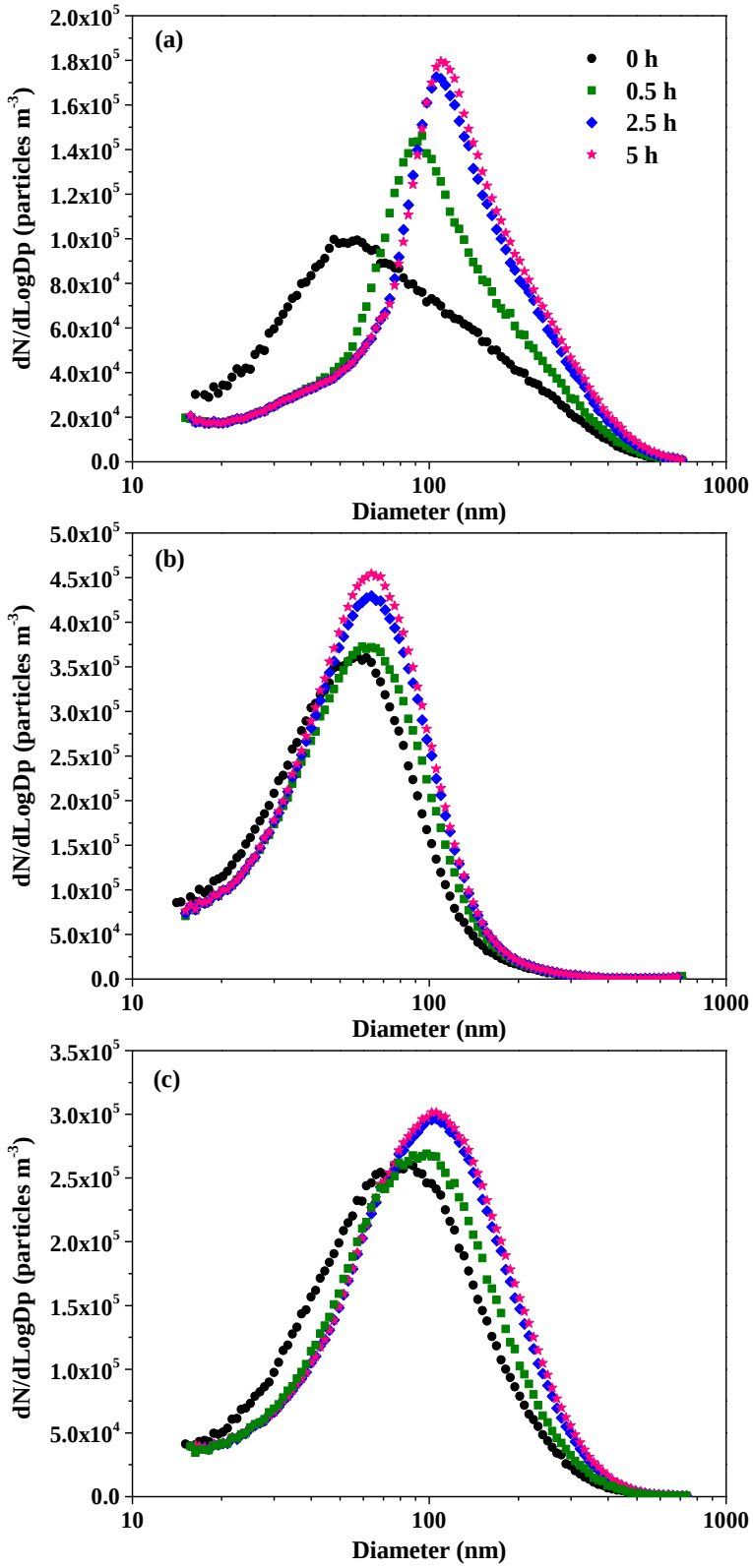

1134

1135 **Figure 3.** Particle size distributions in different burning. (a) Burn 2: rice straw; (b) Burn 3:

1136 corn straw, (c) Burn 5: wheat straw.

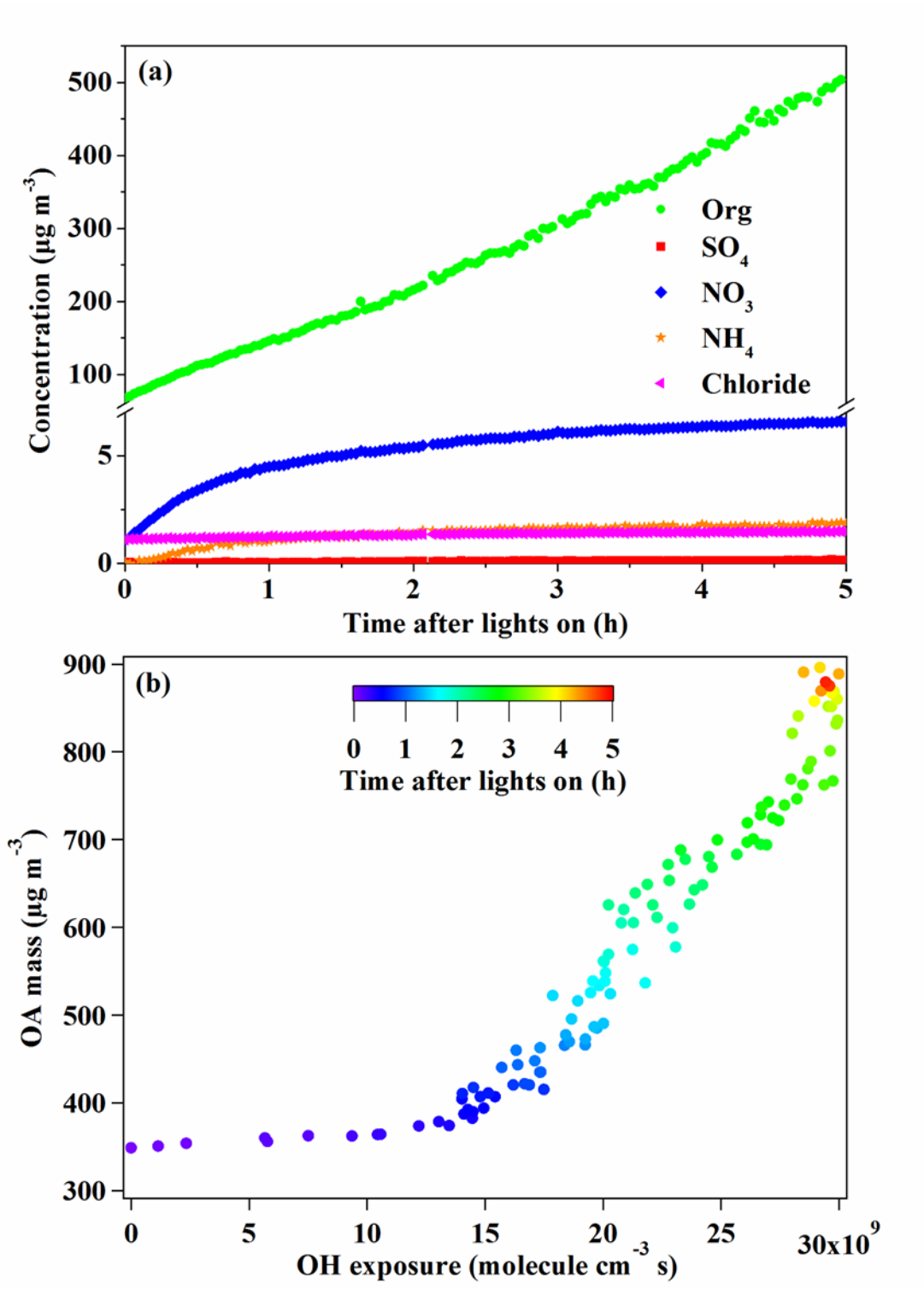

1137

1138 **Figure 4.** (a) The evolution of particulate matter components (Burn 2). (b) OA mass growth as

1139 a function of OH exposure (Burn 5).

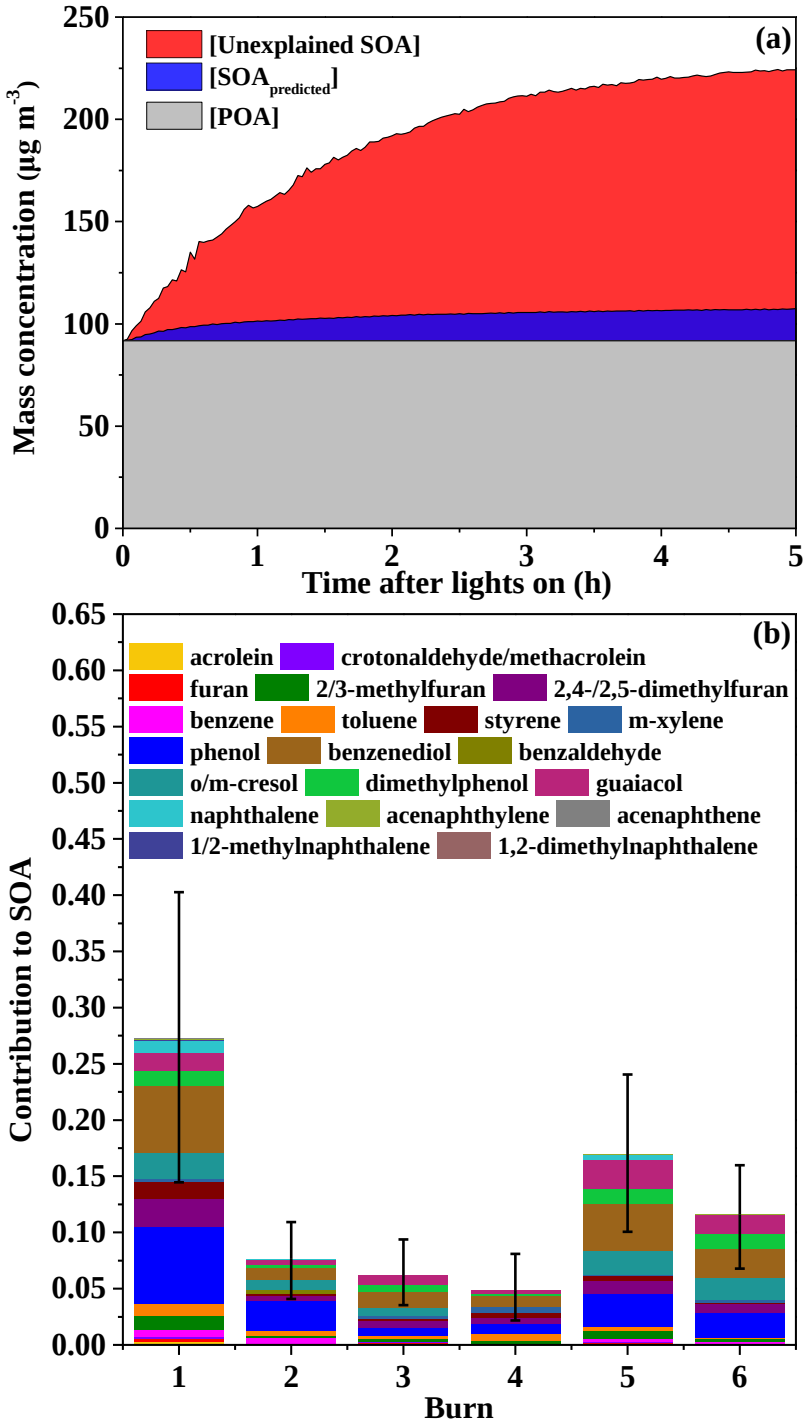

Figure 5. (a) Time series plots of concentrations of POA, secondary organic aerosol that can be explained by the reacted precursors ($SOA_{predicted}$), the difference between the formed SOA and the predicted SOA (Unexplained SOA) in Burn 6. (b) Contribution of 20 NMOGs to the formed SOA at the end of photoreactions. Error bars correspond to the range of contributions when the lowest/highest SOA yields in references were used for all precursors.

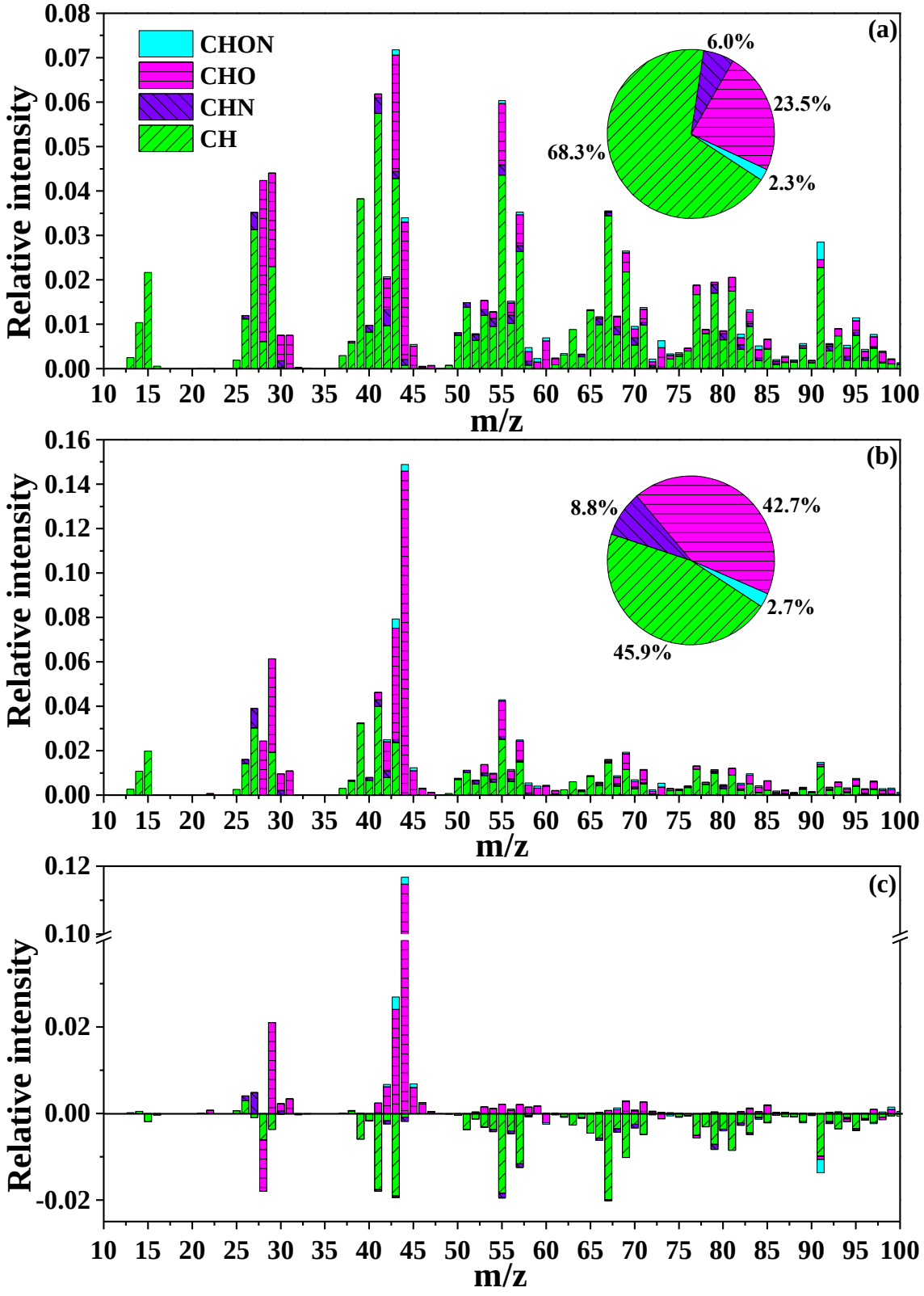

Figure 6. (a) Mass spectrum of POA; (b) mass spectrum of aged OA; (c) Difference in mass spectra between aged OA and POA. The data were all taken from Burn 5.

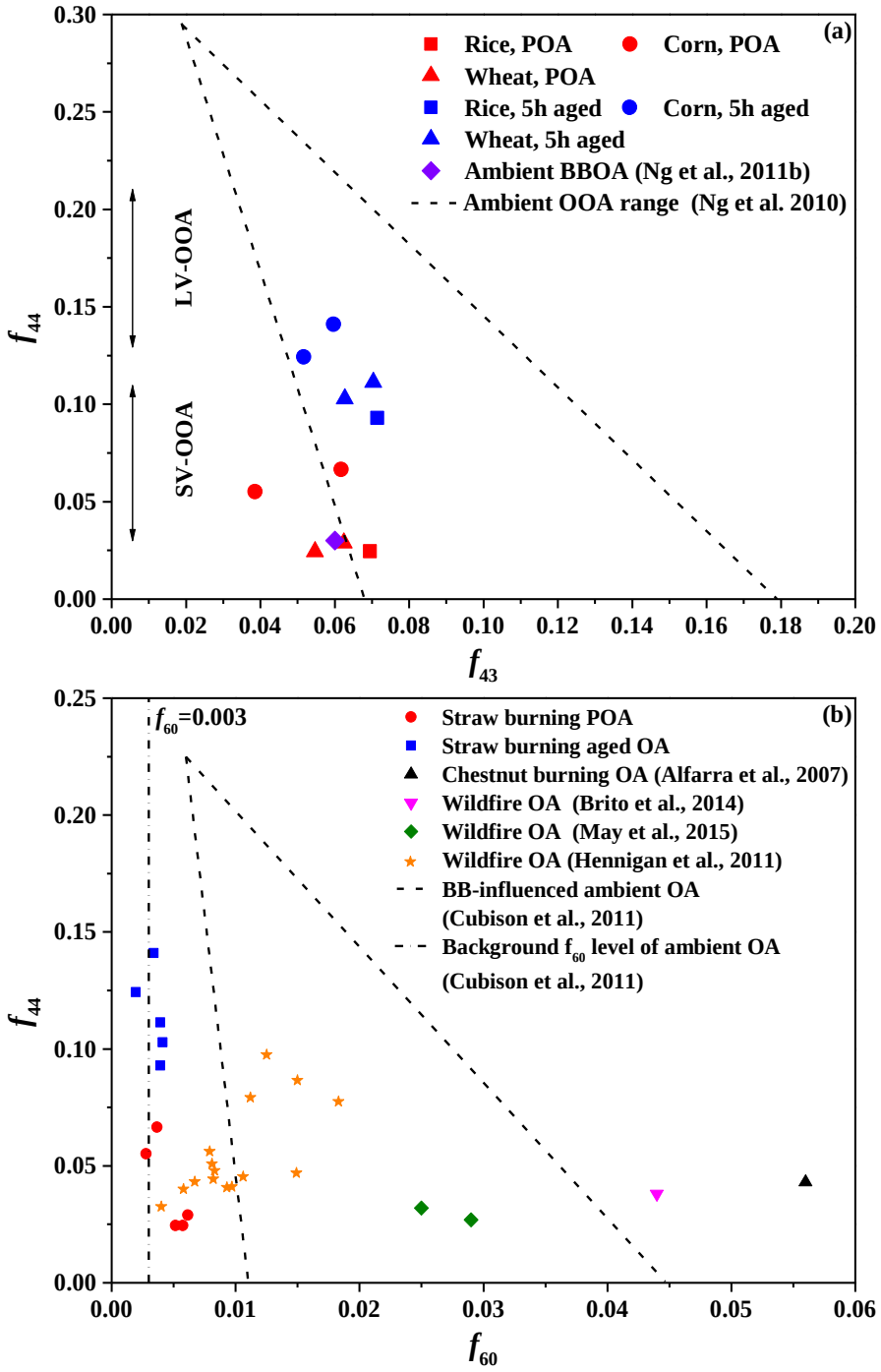

Figure 7. (a) Comparison of f_{44} vs f_{43} determined in our work with those for the ambient BBOA data sets (Ng et al., 2011b) and the ambient OOA range (Ng et al., 2010). The typical f_{44} ranges of ambient SV-OOA and LV-OOA are indicated with the vertical arrows. (b) Comparison of f_{44} vs f_{60} for straw burning OA with those for other types of biomass burning OA (Alfarra et al., 2007; Hennigan et al., 2011; Cubison et al., 2011; Brito et al., 2014; May et al., 2015).

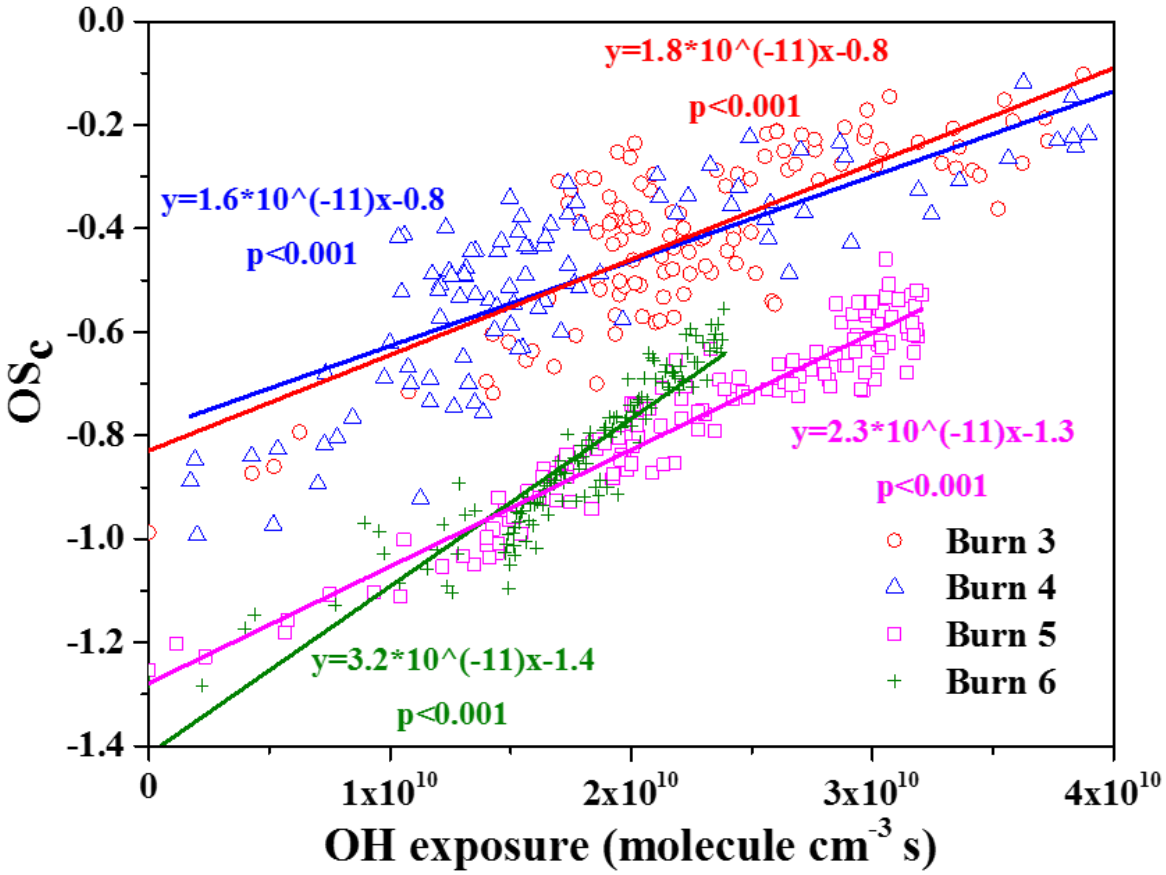

Figure 8. The growth of OA carbon oxidation state with OH exposure for burning corn (Burn 3 and 4) and wheat (Burn 5 and 6) straws. Data for burning rice straws were not included since in Burn 1 AMS was then not run in W-mode.

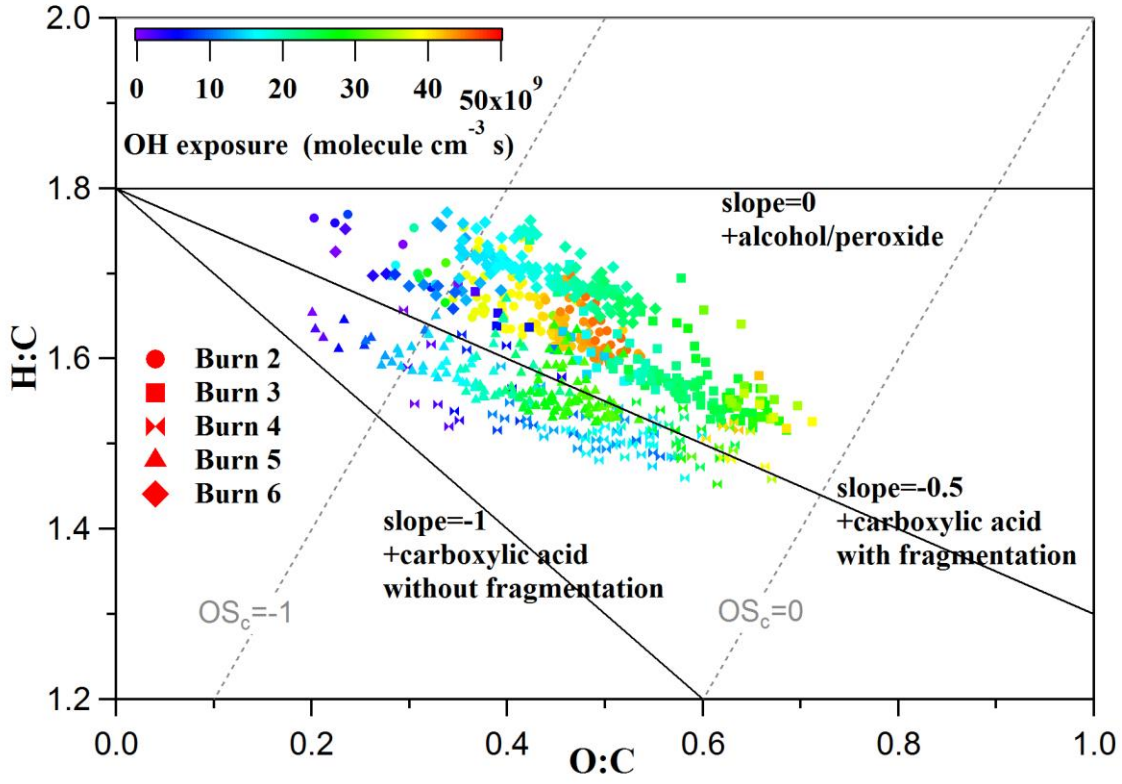

1159

1160 **Figure 9.** Van Krevelen diagram for the OA. Each slope corresponds to the addition of a

1161 specific functional group to an aliphatic carbon.

1162